027117

Volume II

Final Report for

Applications in Astronomy Suitable for Study by Means of Manned Orbiting Observatories and Related Instrumentation and Operational Requirements

Edited by

Laurence W. Fredrick

Supported by NASA Grant No. NsG-480

LEANDER McCORMICK OBSERVATORY
UNIVERSITY OF VIRGINIA ○ CHARLOTTESVILLE

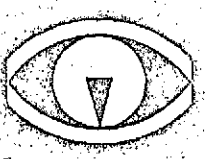

Reproduced by
NATIONAL TECHNICAL
INFORMATION SERVICE
US Department of Commerce
Springfield, VA. 22151

NASA-CR-112285) APPLICATIONS IN ASTRONOMY SUITABLE FOR STUDY BY MEANS OF MANNED ORBITING OBSERVATORIES AND RELATED INSTRUMENTATION AND OPERATIONAL (Leander McCormick Observatory) 87 p

N73-72436

Unclas
00/99 67862

Volume II

Final Report for

Applications in Astronomy Suitable for Study by Means of Manned Orbiting Observatories and Related Instrumentation and Operational Requirements

Edited by

Laurence W. Fredrick

Supported by NASA Grant No. NsG-480

1963

Volume II

Contents

Part II

Introduction

In the following part of this report we have reproduced in pre-publication form, papers on various topics and side topics essential to the discussion in Part I of this report. Some of these papers are essentially compilations or condensations of well-known problems. Some are brief elaborations of subjects and some are original papers, the work appearing here for the first time. We plan to publish these original papers in the near future.

Paper I

Accuracy of Masses

by L. Fredrick and D. MacDonald

One of the most essential parameters in astronomy is the mass of a star. The only reliable method for determining mass is from double stars and for certain pairs (0".1 to 1".5) we are forced to rely upon visual observation with its resultant inaccuracy. For unresolved pairs or large magnitude differences we determine, from astrometric or spectroscopic observations, only a mass function. We are therefore concerned with determining or improving masses.

The essential relations are:

$$M_1 + M_2 = a^3/P^2 \qquad (1)$$

$$M_1 a_1 = M_2 a_2 \qquad (2)$$

$$V_1 M_1 = V_2 M_2 \qquad (3)$$

These relations contain seven parameters (since $a_1 = a_2 = a$) and are given in solar mass units, astronomical units, and kilometers per second. In many cases we observe $\underline{a}$ in seconds of arc and it is therefore required that we know the parallax π and the inclination of the orbit to obtain the true $\underline{a}$ values needed for equations (1-3) above.

Double stars may be tabulated in the following manner:

1. Astrometric
   a. Resolved
   b. Unresolved (blended image)
   c. Unresolved (single image)

2. Spectroscopic
   a. Double line
   b. Single line
   c. Blended line

3. Eclipsing
   a. Primary only
   b. Primary and secondary

Since it is apparent that spectroscopic binaries cannot yield the masses unless the inclination is known, we will consider them only when they contribute to the other cases.

Only in the astrometric resolved case where a parallax is available do we actually obtain the masses without resort to the other methods. However, in many cases we must appeal to the other methods and in some cases to all three, in order to get the masses. In all cases these masses are obtained to varying degrees of accuracy (or lack of accuracy).

$$dM_{1,2} = (M_1 + M_2)\left(\frac{3da}{a} + \frac{3d\pi}{\pi} + \frac{2dP}{P}\right) \qquad (4)$$

We see immediately, that in the interesting cases, P is known with sufficient accuracy and that a and π are the real culprits. Thus any observations that improve either of these are highly desirable. This is especially important for $\underline{a}$ since it enters again through equation (2).

A particularly interesting case is where a system is classed as an astrometric and eclipsing binary. Here we know P with such precision that dP is essentially zero.

Another special case is a system that falls in classes 2 and 3 . Since, in this case we stand to observe a(and a_1 and a_2) with great precision as well as P, these should yield even more accurate masses. However, in the simple case we derive that:

$$M_1 + M_2 = ZPV^3 \qquad (5)$$

where Z is a lumped constant, P is the period in seconds and V is the orbital velocity of one star to the other in kilometers per second. In the best cases, even though P remains accurately known, V enters by a factor of three in the accuracy of the masses since,

$$dM_{1,2} = (M_1 + M_2)Z\left(\frac{dP}{P} + \frac{3dv}{v}\right) \qquad (6)$$

If we treat the methods of observation we come upon this immediate fact. So far as double stars are concerned, there is no need to observe v_1 , v_2 , and P from orbit. These quantities are obtainable with equal accuracy from the surface of the earth. The only advantage an orbiting telescope has for these three quantities is to push v_1 and v_2 to fainter systems(which is an advantage). It is equally immediate that for practical purposes we cannot improve upon the values of π by means of satellites, at least for the time being. All that is left is to improve $\underline{a}$.

The resolution of a ground based telescope is limited by the seeing disk to about 1.0 seconds of arc. Thus, except for light gathering power there is no reason for building a telescope much larger than 40 inches diameter. Now, because of emulsion effects and the

like the photographic method is valid for separations down to about 1".5. Extrapolating, we find for a telescope resolving 0.05 seconds and not seeing limited that we should photograph separations of about 0".07. We are ignoring the existence of large differences of magnitude between the components.

A list of a few selected astrometric binaries, only one of which is resolved on the plate, is given in Table I.

Table I

Star	Period	Separation	Parallax	Error in M
13 Cet*	6^{y}95	0".236	".063±4	100%
9 Pup	23.18	0.58	.67 4	100
ζ CncAB	59.7	.88	.047 5	
10 UMa	20.8	.61	.073 4	
η CrB	41.62	.91	.065 6	
Mel 4 *	42.09	1.82	.142 7	40
β Del	26.6	.48	.032 5	
δ Egl	5.70	.26	.052 4	60
K Peg	11.405	.336	.036 3	
BD-8°4352*	1.715	.218	.157 3	100

From this table we see immediately that poor masses are associated with small separations and small parallaxes. However, the masses of four systems should be better than is indicated. These stars are marked by asterisks. Much of the difficulty lies in a and observations of this parameter will leave all of the uncertainty to the parallax. Table II gives a list of interesting stars for this work and Table III lists a set of the most interesting stars which have faint companions not yet observed by astrometric techniques.

The operational requirements are based upon the observing

technique used. If we use a photographic plate as in the Herzberg technique and require many exposures per plate, we require guiding accuracy to about the image size. Actually, we prefer guiding to one half the image size which would be 0.03 to 0.04 seconds of arc. This is a stringent requirement and any relaxation of this raises the level of the smallest observable separation. Setting accuracy need only be to 0.5 minutes of arc.

An automatic plate holder would change the plates and make the exposures. Changing of the plate load would depend upon the capacity of the plate holder. Each star might require 1/2 hour operational time so the telescope would have to be re-set at 1/2 hour intervals on a new star.

Table II

Star	P	Axis	Separation	Parallax	
Melb 4AB	42.09	1.82	-	0.142±.005	
26 DRA	74.16	1.50	-	0.073	4
ζ HER	34.38	1.369	-	0.103	4
μ HER BC	43.02	1.287	0.08	0.109	6
β 648	59.8	1.26	1.31 (1960)	0.059	4
Ross 614	16.5	1.1	0.9	0.251	3
99 HER	56.40	1.03	1.41	0.058	4
ψ VEL	34.11	0.920	-	0.062	6
η CRB	41.62	0.907	0.68	0.065	6
ζ CNC AB	59.7	0.88	1.14	0.047	5
τ CYG	49.8	0.85	0.81	0.047	3
85 PEG	26.27	0.83	0.75	0.83	4
FU 46	13.12	0.71	-	0.147	7
10 UMA	22.20	0.61	0.55	0.074	3
9 PUP	23.18	0.58	-	0.060	4
β DEL	26.6	0.48	0.17	0.032	5
K PEG	43.02	0.336	0.12	0.036	3
M ORI	17.5	0.276	0.24	0.028	6
HO 581	25.69	0.27	0.18	0.018	4
δ EaV	5.70	0.26	0.10	0.056	4
13 CET	6.95	0.236	0.13	0.058	5
BD-8°4352	1.715	0.218	0.27	1.57	3
α AUR	0.2847	0.0559	-	0.074	3

Table III

Stars with Invisible Components of Small Mass

Star	RA	Decl
η CAS A	0 46 03	+57°33.1
o^2 ERI A	4 12 58	- 7 43.8
Ross 434	9 41 29	+76 17.3
Wolf 358	10 48 19	+ 7 05.1
Lalande 21185	11 00 37	+36 18.3
BD + 11°2625	14 10 05	+11 01.4
Proxima Cen	14 26 19	-62 28.1
ξ Boo A	14 49 05	+19 18.4
ADS 10598 A	17 27 49	- 1 01.4
μ Her A	17 44 30	+27 44.9
Barnard's Star	17 55 23	+ 4 33.3
70 Oph A	18 02 56	+ 2 30.6
Ci 1244	19 20 37	-59 55.1
δ Aql	19 22 59	+ 3 00.8
61 Cyg A	21 04 40	+38 30.0

References

Gliese, W., Astron. Rech-Inst., Heidelberg, Mitt. Series A No. 8, 1957

Harris, D. L. et. al., Basic Astonomical Data, p. 273 University of Chicago Press, 1963.

Strand, K. Aa and Hall, R. G., Apj. 120, 322, 1954.

van de Kamp, Peter, AJ 59, 447, 1954.

Paper 2

The Use of Large Orbiting Telescopes for Cosmological Tests

by D. Meisel

The uniform models of the universe based on general relativity and the observational tests of them have been known for over 30 years. Yet, there still remains quite a lot of observational work to be done before any particular model can be given preference.

The term uniform means that the "overall" distribution of matter is a perfect fluid with its pressure and density independent of spatial coordinates and functions of time only.

These models must be regarded as crude approximations to reality since the largest observable units of organization tend to cluster (i.e., galaxies). They are useful in that their properties can be calculated rather easily and observational tests made (McVittie, 1956).

The metric of a uniform cosmological model is given by McVittie (1956) as,

$$ds^2 = dt^2 - \frac{R^2(t)}{c^2}\left\{\frac{dx^2 + dy^2 + dz^2}{(1 + kr^2/4)^2}\right\}$$

Where R and K are parameters which must be found experimentally.

It can be shown (McVittie, 1956) that this metric leads to three different definitions of distance: a) size distance,

b) luminosity distance and c) the volume distance. The luminosity of size distance can be related to the amount of observed red shift by appropriate equations. Many attempts have been made in recent years to try to find K and R for the metric. This is extremely difficult to do in any case. It is possible, however, to make relative measurements and determine if the universe is indeed a good fit to the uniform model, and if so, which model.

1. Luminosity Distance
   The luminosity distance of distant object is given by,

$$\frac{D}{D_s} = \left(\frac{1+\delta}{1+\delta_s}\right) \frac{1+x}{2} \left(\frac{S_s}{S}\right)^{1/2}$$

Where D is the luminosity distance, S is the signal strength of the source, x is the exponent of intensity-frequency variation in the wavelength range ($\lambda_1^1 = \lambda_1 + \Delta\lambda$ to $\lambda_2 = \lambda_2 + \Delta\lambda$) at the source, and is the red shift $\Delta\lambda/\lambda$. The subscript refers to some particular standard object. The x value is the slope for the wavelength range and may be found from nearby objects which have low relative velocities. (λ_1, λ_2 are the observed; λ_1^1 λ_2^1 are unshifted.)

2. Size Distance

The theory of relativity requires that the null geodesic be assigned to the path of a photon. This means that the distance obtained from the inverse-square law of radiation will be different,

in general, from that obtained by triangulation of size. McVittie (1956) shows that,

$$\xi = D/(1+\delta)^2$$

Where ξ is the distance given by $\phi = \xi\theta$, where ϕ is the linear diameter of the object and θ is its angular diameter. If the object under consideration has small angular size, then their angular sizes and distances are related by,

$$\theta_1/\theta_2 = \xi_2\phi_1/(\xi_1\phi_2) \text{ or } \xi_2/\xi_1 = \theta_1\phi_2/(\theta_2\phi_1)$$

If a standard has a certain diameter ϕ_s and a corresponding angular diameter θ_s the relation becomes,

$$\xi/\xi_s = \theta_s\phi/(\theta\phi_s)$$

If $\phi_s = \phi$ then, $\xi/\xi_s = \theta_s/\theta$

Substitution gives a relation between size and brightness,

$$\frac{\theta}{\theta_s} = \left(\frac{1+\delta}{1+\delta_s}\right)^{\left(\frac{x}{2}-\frac{3}{2}\right)}\left(\frac{S}{S_s}\right)$$

The average surface brightness is given by,

$$\frac{B}{B} = \left(\frac{1+\delta}{1+\delta_s}\right)^{x-3}$$

In other words, surface brightness is no longer <u>independent</u> of distance.

The mean surface brightness is given by,

$$B = \frac{\int_0^\infty \int_0^{2\pi} I(r,\phi) r d\phi\, dr}{\int_0^\infty \int_0^{2\pi} r d\phi dr}$$

Where r, ϕ are apparent coordinates on the surface of the object.

~~3. A Test of Uniformity~~

The brightness relation gives an important means of testing

the concept of uniformity. Consider two identical sources at different distances. The generalized form of the surface brightness relation is given by,

$$\frac{B}{B_s} = \left(\frac{1+\delta}{1+\delta_s}\right)^{x+\alpha}$$

Where x depends on the luminosity function of the source, α is a constant determined from observation.

If $\alpha = -3$, the model of uniformity applies to the observable universe. If it is different from -3, then some other assumption will have to be made.

The advantage of using surface brightness rather than luminosity or size is that the surface brightness can be found for <u>equal</u> areas on each object.

Since the brightness distribution across the surface is far from uniform the degree of accuracy depends on the ability to resolve distant galaxies and also to make readings of surface brightness. Since low sky brightness is also a necessity here, an orbiting telescope is a distinct advantage. Some of the objects may require also that spectra be taken to determine δ more accurately. The determination of X is probably the main difficulty. All of the objects used to find α must be identical. If the objects are not identical, the relations become,

$$\frac{B}{B_s} = \left(\frac{1+\delta}{1+\delta_s}\right)^{x+\alpha} \left(\frac{\phi_s}{\phi}\right) \left(\frac{\ell}{\ell_s}\right)^2$$

Where ϕ is the actual linear diameter of the source and ℓ is the luminosity of the object, assuming spherical symmetry. The above surface brightness must also be corrected for intergalactic absorption.

4. Selection of Cosmological Models.

The proof of uniformity still does not reveal which cosmological model is the nearest to reality. Neither does uniformity indicate just how expansion is taking place. If it is found that $\alpha = x$ then the expansion models must be abandoned altotether. Since this is unlikely, though possible, it will be assumed that some type of expansion is taking place. If it is found that α is variable with different values of δ and δ_s then the motion cannot be constant velocity or the situation is non-uniform or both.

The information on red shifts and luminosities has been used in the past to attempt to determine the constants which occur in the series expansion of the luminosity distance,

$$D = \frac{c\,\delta}{H}\left\{1+1/2(1-q_o)\,\delta\right\}$$

Where c is the velocity of light and H is Hubble's constant. δ is the red shift and q_o is a constant like H which must be determined from observation.

$$\frac{D}{D_s} = \frac{\delta\left[1+1/2(1-q_o)\delta\right]}{\delta_s\left[1+1/2(1-q_o)\delta\right]}$$

At nearby distances, the values of D are identical to those found on the assumption of Newtonian mechanics. If good reliable distances can be found from the luminosities, then the value of q_o may be found and in turn H can be found also. These are related to the R and K of the metric from which a model may be found. The generalized distance luminosity relation is,

$$\frac{D}{D_s}\left(\frac{1+\delta}{1+\delta_s}\right)^{\frac{X_1-2}{2}}\left(\frac{S_s}{S}\right)^{1/2}$$

Where X_1 is the observational constant.

5. Summary

In order to get the parameters of a near-uniform model universe, the luminosities and intensity distributions over a wide range of wavelengths is necessary to derive X, α , and D which in turn give H and q_o the parameters of the model.

The test for uniformity can be made by comparing the surface brightness of galaxies rather than luminosity in various wavelengths.

If α is not very different from -3 then the near-uniform universe is valid to a fair approximation. If α is not near -3 then uniform models will have to be abandoned and non-uniform models be developed. (McVittie, 1956).

References

McVittie, G. C., Fact and Theory in Cosmology, Eyre and Spottswoode, London, 1961.

McVittie, G. C., General Relativity and Cosmology, Chapman and Hall, London, 1956.

Cosmological Tests

Appendix I

Calculation of the Upper Limit of Detectability of Intergalactic Objects

Assuming the minimum background brightness to be $\bar{I}_v = 0.55 \times 10^{-13}$ ergs cm^{-2} sec^{-1} (sq min)$^{-1}$ this is equal to one 17.5 magnitude star per square second of arc. In the direction of the galactic center, this sky background is about one 21.4 magnitude star per square second of arc.

Using M31 as an example. It has a surface brightness of one 13.3 magnitude star per square minute of arc. Assuming that uniformity holds and Hubble's constant has a value of 75km/sec/kpc. For M31 , the distance is 46kpc and thus $v = 3.45 \times 10^3$km/sec and $\delta = 10^{-2}$. In the visual x is effectively 0. And thus,

$$\frac{B}{B_s} = \left(\frac{1+\delta}{1+\delta}\right)^{-3}$$

$$B/B_s = 0.02 = (1+\delta)^{-3} \text{ or } \delta = 5$$

Hence if the galaxies were all of the surface brightness of the Andromeda galaxy, the sky brightness would not interfere at the galactic pole out to $\delta = 5$. In the region of the galactic plane $\delta = 1.15$ is the limit.

According to McVittie (1956) the theoretical limiting value of δ is 1.133. So if one ignores absorption by dust in space itself then there is no limitation imposed by sky background above.

100 mile altitudes.

If it is not possible to see out to distances for $\delta = 1.133$ then dust must be responsible. If it is possible to see beyond $\delta = 1.133$ then the model can be assumed not to be valid.

The limit of operation is a matter of integration time rather than inherent difficulty. Since dust is present, it is doubtful that the limiting factor will be sky background or integration time, but the actual scattering of light.

Paper 3

The Study of Galactic Nebulae and Diffusing Matter

by D. Meisel

Proposals for studying the spectra of galactic nebulae in extreme wavelength regions have already been advanced by various investigators. Most of these utilize narrow field telescopes that examine small fields of view.

With a very large telescope having a nominal of view, it should be possible to obtain high resolution, monochromatic photographs of large structures in the galaxy over a wide range of wavelength. These photographs would be useful in studies of the following objects and phenomena.

1) Shock wave phenomena in new and old novae and supernovae explosion envelopes.

2) The study of minute dark nebulae visible against the galactic background.

3) The discovery and study of nebular complexes in nearby galaxies and star systems.

4) Investigations of shock wave structures in normal emission nebulae in order to determine the presence and strength of galactic magnetic fields.

5) Aid in the discovery of dust laden areas of the galactic structure and the interpretation of stellar polarization. (see later paper by author on star comets)

6) The determination of relative positions of superposed nebular structures on the basis of the degree of interstellar reddening that exists.

7) The redetermination of the absorption coefficients for complex regions of the galaxy.

With an auxiliary telescope of short focal ratio and moderate aperture, the whole Milky Way could be covered in five different wavelengths from the UV to the far infrared (using image tubes of large diameter) within a time space of several months. Objects of interest could be then be studied in detail with the large aperture telescope. The information gained from such a survey would be of value in studies of galactic structure and would supplement current radio studies and O and B association surveys.

Paper 4

The Search for Very Cool Stars Using a Large Orbiting Telescope

by John T. Carter

Part I - The Hayashi Theory

Prior to recent work by Hayashi (1962), it was believed that the time scale for the Helmholtz-Kelvin contraction of stars of low mass ($M < 0.1 M_\odot$) was greater than 10^{11} years. This belief was based on the assumption that the contracting stars evolved horizontally on the H-R diagram. However, Hayashi's theory of the convective nature of these stars during contraction results in a much shorter ($<10^9$ years) contraction time along a vertical path on the H-R diagram. Using Hayashi's theory, Kumar (1963) derived the following time scale for the H-K contraction of stars of low mass:

$$t_{H\text{-}K} = 4.98 \times 10^9 \times \frac{M}{T^4 R^3}$$

where M and R are the mass and radius in solar units, and T is the effective temperature in thousands of degrees Kelvin. According to Kumar, stars of mass $M \leq .07 M_\odot$ would never evolve to the main sequence, but rather would become degenerate bodies.

At first glance it would appear that a large number of these bodies would be detectable, since it seems intuitively easier to accumulate a small mass of dust and gas rather than the large masses required for main sequence stars. However, the number

of such detectable bodies would be limited by two factors. In another section of this report infrared techniques were applied specifically to these low mass bodies, and limiting distances for detection were determined. A 2000°K body of radius $R = R_\odot$ would only be detectable at a distance of approximately 100 light years by a telescope of 150" aperture (assuming that the telescope is in orbit). The second limiting factor is the very short time scale. Using the above formula derived by Kumar, it would only take 1.5×10^6 years for a body of mass $M = .07 M_\odot$ to contract to a radius $R = R_\odot$. This would imply that these bodies could only be observed in regions in which star formation has occurred within about one million years. But O and B stars evolve to the main sequence and off it in less than 10^6 years, so there would be a chance of finding these bodies in a region containing O and B stars. However, the author is unable to even make an educated guess as to the number of these bodies.

Care must also be taken to insure that all objects detected in any single detector search system are Hayashi objects. There are two ways to do this. One is to use automatic discriminating devices at other wavelengths, the other is to use a polarimetry survey. Both have their merits and are discussed in this report. The discriminatory system is discussed in the next part of this

paper. The polarimetry method is discussed briefly in paper no. 6.

Part II - Methods of Detection

Recent work by Hayashi (1961) on the convective properties of early stars, and the extension of Hayashi's theory by Kumar (1963) to stars of low mass($\leq .01M_{\odot}$) indicate that there may be a number of stars with a temperature of around 2000°K which never evolve to the main sequence. Such a star would move down the H-R diagram, eventually becoming a completely degenerate object or a black dwarf. Such a 2000° body would be difficult to detect in the visible spectrum since it would only have about 1% of its total power emission in the visible region of the spectrum. However, the peak of the 2000° blackbody curve occurs at 1.45μ and thus the near infrared would be the region in which to look for such a star. The discovery of a number of such stars would tend to support Hayashi's theory on the convective nature of stars during their evolution to the main sequence. The remainder of this report will be a discussion of detectors and a calculation of the necessary photon flux from the stars.

Photoconductuve detectors are generally used in the near infrared region of the spectrum, but there are a number of choices among the photoconductors.

The first choice in general type is that between single crystal

form consists of a slice 1 mil thick, of a single crystal which is then mounted on a substrate. The thin film is produced by chemical precipitation or vacuum sublimation of a thin film on a substrate. In general, the single crystal type is more desirable. The thin film has point to point nonuniformities and is less reproducible. They are more susceptible to damage, may exhibit double time constants, and are always limited by current noise at low frequencies, whereas some single crystal ones are not limited by current noise.

The second type classification is by extrinsic and intrinsic detector material. In an intrinsic substance photons produce a free electron-free hole pair by direct excitation across the forbidden gap. This requires a material having the proper forbidden gap for the spectral response required. In an extrinsic material photons produce a free electron-bound hole or a bound electron-free hole pair by excitation of an impurity level. This achieves a spectral response through use of a doping element having the proper excitation energy. The intrinsic detector generally exhibits fewer detrimental qualities than the extrinsic one. The extrinsic detector requires a very careful doping process, while the doping, if done, of the intrinsic detector, need not be as precise. The extrinsic has a general lower responsitivity and "washed out" optical absorption. However, the number

of narrow energy band semiconductors is somewhat restricted, whereas a wide variety of doped materials having small excitation energies exist.

The actual performance of a given detector can be influenced by a number of factors. The doping of the detector determines the resistivity which in term determines the amplifier system to be used. The size and shape of the sensitive area along with its housing and temperature of operation control its performance characteristic. These problems are discussed in books by Smith, Jones, and Charmar (1957) and Kruse McGlauchlin and McQuistan (1962) and in technical publications by Gelinar and Genoud (1959) and Merrian and Eisenman (1962).

There are only a few materials with peak responses in the region in which the author is interested (1 to 3μ). Lead sulfide is the most commonly used one. It is used as an intrinsic thin-film photoconductor with its peak response coming at 2.1 to 2.5μ depending on the operation temperature and having a cutoff at 2.5 to 3.3μ(longer wavelengths correspond to lower temperatures) at 2μ PbS is superior to all other detectors. The second class of detectors of interest are the germanium and Ge doped detectors. The germanium is of particular interest because of the intrinsic peak at 1.5μ. This response peak is higher than any other that the author has found covered in the literature, but

It is quite narrow (the full width at half maximum being < 1μ). However, the doped Ge detectors have secondary peaks which are lower but much wider. Thus, to cover a wider region of the spectrum, but still have a large response in the peak of the 2000°K black-body curve, a doped Ge detector would seem to be desirable. If the peak alone is desired, then intrinsic Ge could be used. Detector properties in general are discussed in the book by Kruse et. al., and the performance of individual detectors is discussed in a series of technical bulletins by Naugle, Merrian and Eisenman, out of the Naval Ordnance Lab. Corona.

Photon Flux Calculations

The detector noise will be due to two causes, the sky background and intrinsic detector noise. The sky background was calculated by David Meisel in another part of this report and at 1.45μ it would be 5×10^3 photons $sec^{-1} ster^{-1} A^{-1} cm^{-2}$. If one considers a 0.1μ spectral spread, then the flux from one square minute of sky would be 0.42 photons sec^{-1} (sq. min.)$^{-1} cm^{-2}$. Assuming a 150" telescope the flux incident on the detector would be 4.8×10^4 photons sec^{-1} if the field of view is one square minute. A very good detector may have a noise equivalent power of 10^{-12} watts $(cps)^{-1/2}$. Assuming an amplifier with as narrow a bandwidth as that described by Humphreys and Paul (1963) the NEP would be about 10^{-13} watts. One watt is 10^7 ergs sec^{-1} and at 1.45μ

one photon has an energy of 13.6×10^{13} ergs, so the NEP would be approximately 7.4×10^{5} photons sec^{-1}. The total noise can be approximated by the sum of these two noise sources and thus would be about 8×10^{5} photons sec^{-1}.

The peak power output of a 2000°K blackbody occurs at 1.45μ and it is 40 watts cm^{-2} sec^{-1}. Assuming a 0.1μ response band, the intensity would be 3×10^{19} photons sec^{-1} cm^{-2} at the surface of the blackbody.

Table I gives the intensity at the surface of the earth for stars of radii 2, 10 and 50 R⊙ at distances from the earth of 10 light years and 10 parsecs.

Table I

10 light years	6.6×10^{3}	1.6×10^{5}	4.1×10^{6}
10 Parsecs	6.2×10^{2}	1.5×10^{4}	3.8×10^{5}

(Flux in photons $sec^{-1} cm^{-2}$).

The noise equivalent flux determined above was 8×10^{5} photons sec^{-1}. If one assumes that a minimum signal to noise ratio of two is needed, then the flux from a star must be greater than 16×10^{5} photons sec^{-1}. Table II gives the maximum distances at which stars of the three diameters should give a sufficient flux assuming a collector of 150" diameter.

Table II

Star Radius	Maximum Distance
12 R⊙	210 light years
10 R⊙	1050 " "
50 R⊙	5250 " "

According to Hayashi's theory, there should be a number of 2000°K bodies within these distances. These maximum distance values are directly proportional to the telescope diameter. Thus if a 75" telescope were to be used, the maximum distance for a detectable star of 2 $R_\odot$ and temperature 2000°K would be only 105 light years.

References

Gelinar, R. W. and Genoud, R. H., Rand Report, p. 1697 (May 11, 1959).

Hayashi, C. (1961), Pubs, Astro, Soc., Japan 13, 450.

Humphreys, C. J. and Paul, E., Jr. (1963) Applied Optics 2, 691.

Kruse, McGlauchlin and McQuistan, Elements of Infrared Technology, John Wiley and Sons, New York (1962).

Kumar, S. S., On the Nature of the Planetary Companions of Stars, a publication by Goddard Institute for Space Studies, (1963)

Merrian, J. P. and Eisenman, W. L. Interpretation of Photodetector Parameters, NOLC Report 558 (Jan. 15, 1962).

Naugle, A. B., Merrian, J. P., and Eisenman, W. L. Properties of Photodetectors, a series of NOLC Reports

Smith, Jones, and Chasmar, The Detection and Measurement of Infrared Radiation, Clarendon Press, Oxford (1957).

G_e Detector References

The following technical reports have data on individual G_e detectors. A C indicates a classified report and a U indicates an unclassified one.

G_e (Intrinsic)
NBS 30-E-118, 1953. C
NOLC 279, 1955. U

G_e (Au-Doped)
NOLC 210, 1955, C
" 278, 1955, C
" 360, 1957, C
" 387, 1957, C
" 497, 1960, U
" 525, 1960, U
NAVWEPS 7181, 1961; U

G_e (Cu-Doped)
NAVWEPS 7181, 1961, U
NOLC 557, 1961, U

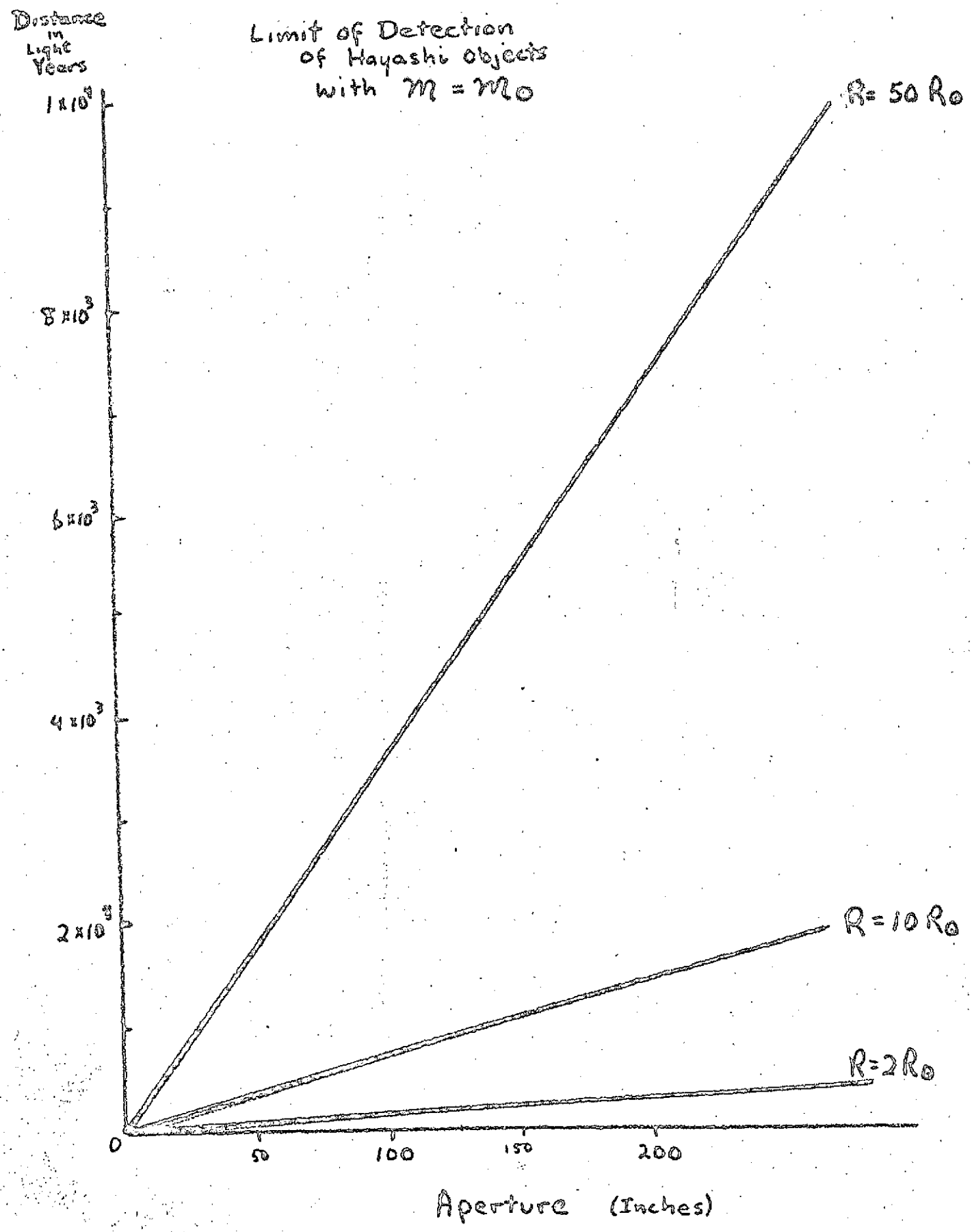
Distance in Light Years
Limit of Detection of Hayashi objects with $\mathcal{M} = \mathcal{M}_0$
1×10^4
8×10^3
6×10^3
4×10^3
2×10^3
0
50
100
150
200
Aperture (Inches)
$R = 50\,R_0$
$R = 10\,R_0$
$R = 2\,R_0$

Paper 5

Stellar Interferometry

by L. Fredrick, G. Borse, and D. Anderson

A problem that has vexed astronomers and taxed their ingenuity as well, is that of stellar diameters. The usual procedure for determining this fundamental quantity has been to obtain all the other quantities and then infer the radius from,

$$L = 4\pi r^2 \, Te^4$$

Michelson and Pease (1921) made a direct attack upon this problem with the now famous beam interferometer and used this instrument to measure the diameters of some six stars. The calculation of the diameters depends upon the parallax and in these cases the errors in the parallaxes are extremely large(several hundred per cent). Another upsetting point in the Michelson and Pease results is the fact that the diameters are scaled inversely proportional to the parallax, an indeed upsetting trend and thought.

Recently Beavers(1956) has tried a variation of the Michelson technique where disappearance of the fringes is not required. This technique however, suffers from moving fringes which may well prove unsurmountable.

A completely different technique has been discussed by Brown and Twiss (1957) and applied to one case (Brown and Twiss, 1958). While at first glance the unusual approach looks promising, a

scrutiny and evaluation of the integration times required shows it to be totally impractical. Therefore, in this note we discuss a modification of the Michelson interferometer employing a 150 inch orbiting telescope.

In the standard interferometer(Michelson, 1927) the procedure is to adjust the phase difference between interferring rays until the respective interference patterns combine to cancel all fringes. The stellar diameter may then be inferred from the theory. However, in order that complete interference be realized optical systems on the order of 20-40 feet must be used. To obtain such separations movable mirrors are usually placed on a long beam. The slightest movement of the mirrors, (half a wavelength or so) will cause the fringes to move. Rapid movement of fringes is a major drawback in such an apparatus. In the proposed interferometer such movement is at a minimum..

The system is illustrated in Figure I and consists of a reflecting circular mirror with four exposed circular surfaces, the remainder of the mirror being blacked out. These four surfaces function similar to the auxiliary mirrors in the Michelson system; however, unlike the latter mirrors, they are not adjustable. Instead , two surfaces are used at a time and two plots of the intensity pattern are obtained. From the ratio of the maximum of the two plots plus the separations of the reflecting surfaces , the radius of the star can be obtained.

An analytical expression for the intensity is obtained as follows:

If the star in question subtends an angle α at the position of the telescope, it can be subdivided into equal elementary strips and each strip is then considered as a point source whose intensity is proportional to the area of the strip. That is, the star is equivalent to a non-uniform line source. Consider next the intensity at P in the focal plane of the objective. In Figure I if M_1 and M_2 are symmetric, the disturbances arriving from different edges of the star traverse paths differing in length by D sin α before they reach the slits and an added path difference of d sin θ from the slits to the point P. Consequently, the disturbances arrive at P with a phase difference δ given by,

$$\delta = \frac{2\pi}{\lambda} \left(D\frac{r}{R} + d\theta\right) \text{ for } \alpha = \frac{r}{R}, \theta \ll 1$$

Where λ = the wavelength of light employed
D = the separation of the mirrors
d = the separation of slits
R = distance to the star
r = distance from center of star to strip considered. r goes from 0 to r_s the radius of star.
θ = angle to point P on screen.

Thus a strip at r gives at P two disturbances whose separate intensities may be represented by $d\alpha$ and whose phase difference is δ. The intensity can be represented by $dI \propto d\alpha(1 + \cos\delta)$ and the total intensity is calculated by integrating over r from 0 to r_s; and the result is :(Longhurst, 1957, p. 220)- $I \propto 1 + 2\cos\left(\frac{2\pi}{\lambda} d\theta\right)\frac{J_1(x)}{x}$

Where J(X) is the first order Bessel function and X = kDd. Since in this apparatus the fringes never disappear, X is much less than 1.22π, the first zero of J_1. For values of $X < 1.5$, a small argument expression for $\frac{J_1(X)}{X}$ can be used. This expression is found to be,

$$\frac{J_1(X)}{X} = \frac{1}{2}(1 - X^2/8), \quad X < 1.5$$

Then for any <u>two</u> measurements of the intensity we have:

$$r_s^2 = \frac{(\frac{I_2}{I_1} - 1)(1 + \cos kd\theta)}{(\frac{I_2}{I_1} D_1^2 - D_2^2)(\cos kd\theta)} 8 \frac{R^2}{k^2}$$

Where $k = 2\pi/\lambda$, for $kDa < 1.5$ and where D_1 and D_2 refer to different zones. The angular separation of the fringes is about 7×10^{-5} radians. Therefore if a value of d is taken as 1/2 cm. and if the distance L from the slits to the screen is 16 feet, we obtain about four fringes per mm. The intensity of these fringes can be scanned by an image orthicon and the intensity values plotted. the maximum value will correspond to $\theta = 0$. Thus if the two maximum intensities are obtained in this manner for the two values of D, the expression for r, is,

$$r_s = \frac{4R}{k} \sqrt{\frac{\frac{I_1}{I_2} - 1}{\frac{I_1}{I_2} D_2^2 - D_1^2}}$$

The use of the orthicon is of great convenience in this case. Using the latest interlaced scan (2000 lines per inch) we would have about 10 TV lines per fringe and could then read out the intensity of the charge on the target directly.

If one requires higher resolution , the photoelectrons can be made to pass through a diverging field and give a magnified (say one fringe per mm) image on the target. This would yield even higher resolution.

References

Longhurst, R. S. Geometrical and Physical Optics, 1957 Longmans, Green and Co., New York.

Beavers, W. I , 1963, Astronomical Journal 68, 273

Brown, R. H. and Twiss, R. Q., 1957, PRS 242, 300 Proceedings of the Royal Society.

Brown, R. H. and Twiss, R. Q., 1958, Proceedings of the Royal Society, 248, 222.

Michelson, A. A. and Pease, F. G., 1921, Astrophysical Journal , 53, 249.

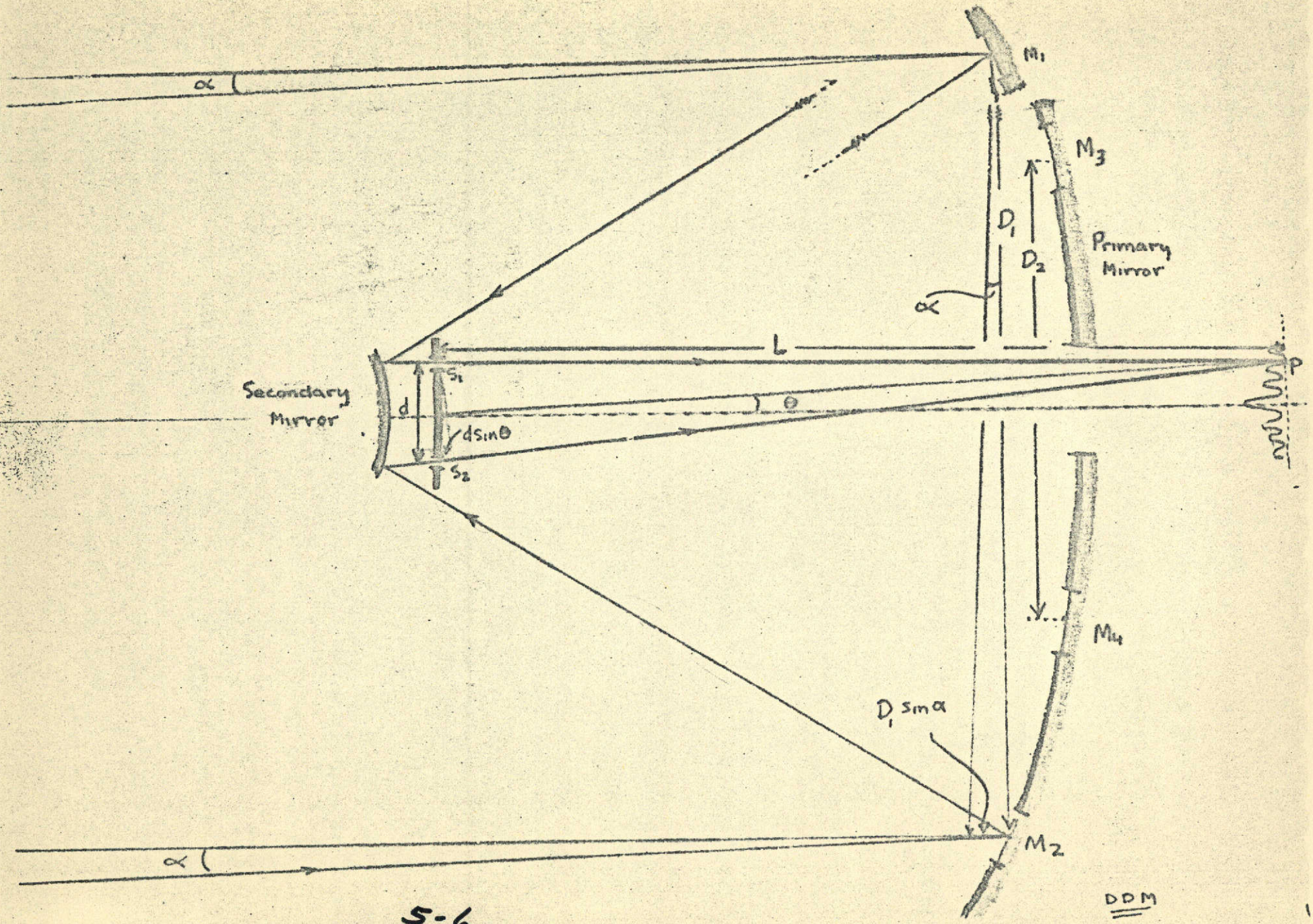
α
M1
M3
D1
D2
Primary Mirror
α
L
P
Secondary Mirror
d
S1
θ
dsinθ
S2
M4
D1 sinα
M2
α

5-6

DDM

Paper 6

On Polarization in Nebulae

by D. Meisel, J. Carter, and L. Fredrick

There are two main sources of polarization in galactic nebulae. One is the polarization due to dust scattering, the other is due to "synchrotron" radiation.

If scattering is the mechanism for polarization, the amount of polarization is related to the absorption coefficient by $p = 0.063A_v$, where A_v is the mean absorption coefficient and p is the polarization in magnitudes (1). Since the absorption coefficient is a function of λ^{-1}, it is assumed that the polarization is also a function of λ^{-1}. Thus in the ultraviolet the polarization should be very high.

The following is a list of selected bright nebulae and the computed polarization for several wavelengths.

NGC or IC	A_V	$\lambda =$ 1500Å	$\lambda =$ 3300Å	$\lambda =$ 5500Å	$\lambda =$ 1.5μ
NGC 1952 (M1)	1.5	0.38	0.147	0.09	0.0135
NGC 1976 (M42)	0.1	0.025	0.099	0.006	0.0009
NGC 1977	0.1	0.025	0.099	0.006	0.0009
IC 434	0.1	0.025	0.099	0.006	0.0009
NGC 2068 (M78)	0.1	0.025	0.099	0.006	0.0009
NGC 2174-5	1.6	0.423	0.165	0.10	0.015
NGC 2237-38-44-46	2	0.532	0.208	0.126	0.0189
NGC 3372	1.0	0.266	0.104	0.063	0.0094
NGC 6514 (M20)	1.0	0.266	0.104	0.063	0.0094
NGC 6523 (M8)	1.1	0.291	0.114	0.069	0.0103
NGC 6611 (M16)	2.4	0.637	0.249	0.151	0.022
NGC 6618 (M17)	3	0.790	0.309	0.187	0.028
IC 5067-68-70	2.5	0.658	0.258	0.156	0.0235
NGC 7000	1.1	0.291	0.114	0.069	0.0103
IC 5146	1.4	0.270	0.145	0.088	0.0132

Using an extrapolation from the radio data (3) the following nebulae should contribute measurable polarizations assumed to be due to synchrotron radiation. Each object is listed with the extrapolated mean percent of polarization, the maximum percent polarization and the identification: (SN = Supernova).

Polarization at 5500 Å

Object	P(%) mean	P(%) max.	Identification
CasB	0.5%	2%	SN I 1572 A.D.
HB9	1.2	5	SN II
Tau A	9	34	SN I 1054 A.D.
Ori	4	15	M42
Gem	2	6	IC443 SN II
Mon	3	10	Rosette Neb.
Pup A	1	5	SN II
2C 1485	0.08	0.3	SN I 1604 A.D.
Sgr	1.1	4	M8
Sgra	6	2	M17
CygX	7	3	ICI 318
2C1725	2	6	SN II
Cyg loop.	2	6	SN II
Cas. A.	25	96	AN II

The polarization at any point is the sum of the two components of polarization.

$$P = P_1 \cos \theta_1 + P_2 \cos \theta_2$$

Where P_1 is the maximum of the local polarization and

$\theta_1 = (\theta - W_1)$ is the direction of maximum polarization and synchrotron radiation and P_2 is the percent due to dust polarization with $\theta_2 = (\theta - W_2)$ where W_2 is the orientation of the polaroid analyzer.

The way to distinguish between the two sources is study the wavelength dependence of the two sources under high resolution. The scattered polarization should obey the relationship.

$$P \propto 1/\lambda$$

But the synchrotron radiation should follow the law $P \propto 1/\lambda^{n+b}(n+b)\neq 1$ analogously to radio emission. Thus monochromatic surveys of various nebulae would help to separate the two sources of polarization.

The intensity equations would seem to indicate that if the emission in the infrared is highly polarized then it is due mainly to synchrotron radiation. If the radiation is virtually unpolarized, the mechanism cannot be due to acceleration due to relativistic electrons.

It is of interest, then, to investigate the polarization of various nebulae over a wide range of wavelengths and in very great detail both photoelectrically and photographically.

Also of interest are polarization studies of near-by galaxies. Such surveys at fairly high resolution might reveal information concerning galactic magnetic fields. Some theories of galactic formation require large magnetic fields and so these surveys could give a check on the relative strengths of the magnetic fields.

Since ordinary planetary nebulae do not show much polarization, such surveys would help to detect supernovae remains in near-by systems.

Finally, a survey in various wavelengths of the known radio galaxies at high resolution would help to clarify current ideas about their structure. With an orbital telescope of large aperture positions of known radio sources could be searched in the infrared in order to make optical identifications. These observations should be carried out with a program of polarimetry so that Hayashi objects (see paper 4) will not be confused with possible infrared galaxies.

References

Allen, C. W., Astrophysical Quantities, 2nd edition, 1963, p. 252.

Ibid, p. 249

Ibid. p. 256

Shklovsky, Cosmic Radio Waves, Howard, 1960

Paper 7

Detection of Extra-Solar Planets

by G. Borse and D. Anderson

The question of whether ther exist stars other than the sun which possess planetary systems, and if so, how many, is perhaps as important as any question in astronomy. The discovery of other solar systems capable of fostering life similar to that found on earth would have important scientific and philosophical consequences. Man's uniqueness in the universe is one unresolved question that has caused great controversy in the past.

Spitzer (1962) proposed an experiment to determine whether the eleven nearest stars similar to the sun possess planets similar to Jupiter. His experiment requires an orbiting three hundred inch telescope and an occulting disc, 75m in diameter in a syncronous orbit 10,000 km from the telescope. In this paper we propose a modification of this experiment which will eliminate the occulting disc and reduce the size of the mirror to 150 inches.

Consider a star at a distance of five parsecs with a planet similar to Jupiter five AU from it. Using Spitzer's figures of 0.5 for the albedo of Jupiter, at half phase the relative brightness is 10^{-9}. The diffraction pattern for a uniform circular aperture of radius R is given by,

$$I(X) = I(o)4\left[\frac{J_1(X)}{X}\right]^2$$

Where $J_1(X)$ is the usual Bessel function of order 1 and,

$$X = \frac{2\pi R \sin\theta}{\lambda}$$

Where λ is the wavelength of the light considered, taken as 5.5×10^{-5} cm and θ is the angular separation of the planet and the star. In this case θ = 1 arcsec. For large X the average value of $J_1^2(X)$ is $\frac{1}{\pi X}$ and $\frac{I(X)}{I(o)} = \frac{4}{\pi X^3}$

If we employ a 150 inch telescope, X = 211.6 and it turns out that the diffraction pattern at the position of the planet is 330 times brighter than the image of the planet. The telescope could be used, or the diffraction can be reduced by reducing the reflectance of the mirror gradually to zero at the rim. We will consider the latter. Since it is the change in the reflectivity of the mirror, (indeed the change is discontinuous at the edge of the mirror) which gives rise to diffraction effects, we seek to make such changes as gradual as possible and eliminate all discontinuities. That is the curve of reflectivity vs. distance from the center should be "very smooth" and it should have zero tangent at zero and at the radius of the mirror. There are many such curves, but only a few are simple enough to take the Fourier transform and get a closed expression for the intensity.

The curves we investigated were a curve due to Sinton, $(1 - X^2)^2$, $(1 - X^4)^2$ and $J_o(XX_o)$ where X_o is the first zero of the zeroth order Bessel function $J_o(X)$. The resulting intensities are as follows:

Reflectivity	Intensity	Average Value(1)	Planet Intensity(2)
$R = 1, 0 < X < 1$ $R = 0, X > 1$	$I_1(0)\left[\frac{J_1(X)}{X}\right]^2$	$I_1(0)\frac{1}{\pi X^3}$	$\frac{3}{1000}$
$R = (1 - X^2)^2$	$I_2(0)4\left[\frac{J_2(X)}{X^2}\right]^2$	$I_2(0)\frac{4}{\pi X^2}$	333
$R = (1 - X^4)^2$	$I_3(0)144\left[\frac{J_2}{X^2}\right]\left[\frac{2J_3}{X^3}\right]^2$	$I_3(0)\frac{144}{\pi X^5}$	8.7
$R = J_o(XX_o)$	$I_4(0)X_o^4\left[\frac{J_o}{\frac{1}{2}X^2 - X_o^2}\right]$	$I_4(0)\frac{33.45}{\pi X^5}$	40

(1) Average Value of I(X) for large X
(2) Intensity of Planet I(X) at X = 211.6.

Where $I_2(0) = \frac{4}{9} I_1(0)$, $I_3(0) = \frac{1}{4} I_1(0)$, $I_4(0) = \frac{1}{8} I_1(0)$

The reflectivity curves are shown in Figure 7-1. It is seen that in this case Sinton's curve is by far the best. However, if the reflectivity of the mirror is reduced "smoothly" such that the curve falls between curve 1 and curve 3, the planet should still be observable. In fact, if Sinton's curve is used, the diffraction pattern is only 10 times brighter than the image of a planet like earth at a distance of 1 AU from the star.

However, as noted by Spitzer, the scattered radiation from achievable surfaces could perhaps exceed the diffracted light. In this paper the scattered light was neglected and further

still valid with scattering present.

Planets such as Jupiter are very bright, however, in the far-infrared and the luminosity of the planet relative to the central star is then only 2.3×10^4. With no variation in reflectivity this gain in brightness is just compensated for by the fact that resolution is poorer at longer wavelengths.

The method described above to reduce diffraction is found to help very little where long wavelengths are concerned. For example with a 150 inch telescope and $\lambda = 30\mu$, with no variations in reflectivity the diffraction pattern is six times as bright as the image of Jupiter. With the reflectivity varied according to $(1 - X^2)^2$ the diffraction pattern is still twice as bright as the planet's image.

We conclude that detection of planets around neighboring stars by the use of a 150 inch telescope whose reflectivity is varied gradually to zero in a predescribed manner is possible if visible light is used and if scattered light from the telescopes' surface is neglected. Table III in paper I of this report lists the most promising stars.

References

Spitzer Jr., Lyman, "The Beginnings and Future of Space Astronomy", American Scientist, (1963) vol. 50, no. 3, P473-484.

Sinton, Wm. "The Amateur Astronomer" Scientific American, August, 1959, p. 70.

Appendix Paper 7

Notes on Apodization

by D. Meisel

In any optical system the diffraction pattern is due to the image at the aperture stop. In normal astronomical telescopes, the secondary is usually made large enough to insure that the aperture stop is the entrance pupil.

For an instrument where the apodization at the entrance pupil is impractical if the aperture stop is a large telescope mirror, it is desirable to make the secondary(or in the case of the proposed design, the tertiary) mirror be the aperture stop.

For the Cassegrain focus, the size of the secondary , which will just gather all the rays for an on-axis image, is $d = \frac{SA}{f}$

A = aperture of primary
S = distance of Cassegrain from focus of
f = focal length of Primary

Any size of diagonal with diameter smaller than d automatically becomes the aperture stop.

Let the aperture of the diagonal be equal to d. The equivalent focal length of the Cassegrain determines the equivalent aperture of the system.

$$A' = \frac{f'd}{\ell} \qquad A' = \frac{f'SA}{f\ell}$$

ℓ = distance of Cassegrain secondary from the system focus.

f'/f = amplification factor = M

$A' = M(\frac{S}{\ell})\ A$ In order to keep A = A'

then $M(\frac{S}{\ell}) = 1$

or $M = (\frac{\ell}{S})$

for f/1 primary

f/25 M = 25 or ℓ = 25 and S = 1.

The apodization curves for the primary mirror may be applied to the secondary in a manner which is straight forward substituting for X, the coordinates of the primary using y, the coordinates of the Cassegrain secondary. The diameter of the secondary is given by:

$$d = \frac{\ell}{M}\left(\frac{A}{F}\right)$$

Note that: $\ell + S = f + h$ where h is the distance behind the main mirror, that the Cassegrain focus lies.

A reflectivity pattern that is symmetrical and should be attempted is:

$$R(X) = 1 + \cos\left(\frac{\pi X}{R_o}\right)$$

Where R_o is the radius of the mirror to be apodized. This should be investigated since it is the only curve which is symmetrical but still possessing the desired end conditions.

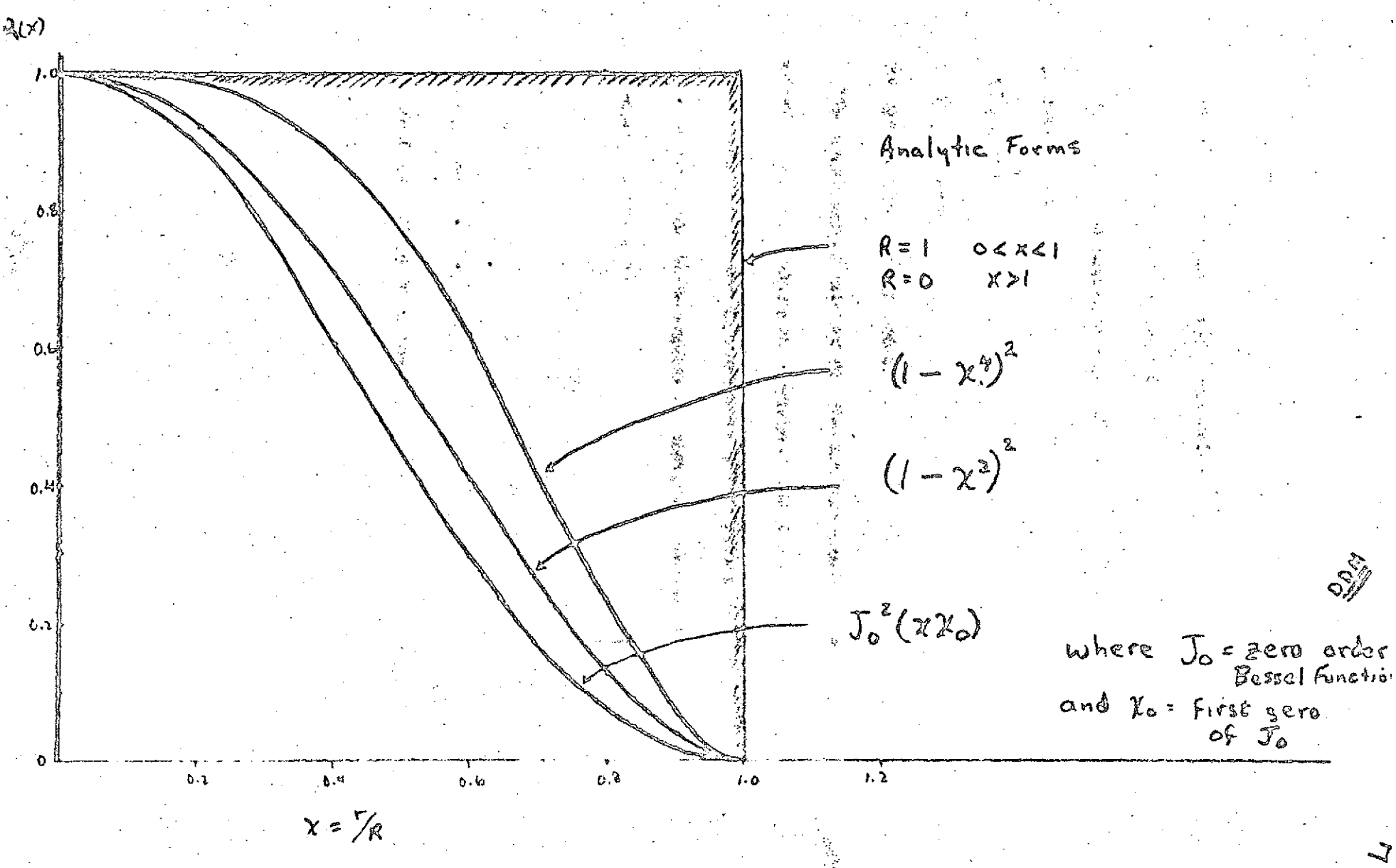

Figure 7-1

Reproduced from best available copy.

Paper 8

Comet Photometry from Orbiting Observatories

by D. Meisel

The principal emission features in the visible and photographic spectral regions of a comet are due to the bands of the organic molecules C_2 and CN with some CO^+ and N^+. In many comets, there is also a faint continuum due to dust reflection of the solar spectrum. On spectra of comets there are three bands which are the most convenient to study:

a) 3883 A band of CN
b) 4737 A band of C_2
c) 4050 A band tenatively assigned to C_3

Some comets show also the bands of CO^+ and N_2^+ but these are confined to the tails of comets rather than the heads.

A recent study by the author(1963) has shown that these bands behave in a manner which is independent of each other, but dependent on the heliocentric distance of the particular comet. Since this study was very limited in scope and accuracy, it would be of interest to do intermediate band photometry of the three bands mentioned above over a wide range of heliocentric distances.

After the band intensities have been obtained as a function of heliocentric distance, these can be used to normalize observed intensities to unit heliocentric distance. The unit intensities of various comets can be intercompared to determing real clemental

abundance differences. The comets, it is hoped, will show abundance differences that are great enough to enable them to be classified.

Also of interest is the relative intensity of the continuum in various spectral regions. These intensities should be calibrated and normalized as were the emission bands. In a first attempt to do this for comets already observed, the author(1963) found evidence for two types of comets which could be correlated with their photometric behavior and unit-distance relative intensities. One type had an abundance of CO^+ in its spectrum. The other type had abnormal CH.

Since the sample was very small(ten objects) the results should be regarded as being extremely tenative. Yet there were indications that the CO^+ comets corresponded to the dust-ice model proposed by Whipple(1952), while the CH comets seemed to correspond to Lyttleton model(1953). In this study there was no correlation between the amount of dust(strength of continuum) and the unit brightness of the comet. Presently held theories about comets require that the amount of dust present is proportional to the total brightness and that the dust is an indication of age. The presence of two types of comets and neither with a dust correlation seems to indicate an entirely different situation.

From an orbiting satellite, the constant monitoring of

comet brightness would also give valuable information about cometary brightness changes induced by solar activity. This would help to tell if the intrinsic brightness variations found by Bobrovnikoff(1941) are real and if correlations of these with cometary type are valid(Meisel, 1963).

If it is found that the two types of comets are real and have different origins, the cosmological implications could be very significant. If it is found that no such distinction exists, then a photometric analysis of comet light free from disturbing influences of the earth's atmosphere will help decide which of the currently held models is valid, if any. It also would help define the law of comet brightness more precisely.

For such a program to be attempted using ground-based equipment, only the brighter objects can be monitored and even then, this can be done usually only for a very short time before and after perihelion. The results are for the most part, continuous and much more reliable.

References

Bobrovnikoff, N. T., Perkins Contribution No. 14 and 15(1941-42)

Lyttleton, R. A., The Comets and Their Origin, Cambridge Press (1953)

Meisel, David D., Masters Thesis, "A Physical Classification System for Comets", The Ohio State University, Columbus, Ohio(1963)

Whipple, F. L. Ap. J. III, 375 (1950).

Paper 9

Proposed Design of an All-Reflecting Schmidt Telescope

by D. Meisel and L. Fredrick

If a telescope is designed to be utilized in astronomical research in the ultraviolet region, it must have no lenses but consist of reflecting surfaces. There are many existing telescopes that fulfill this requirement, but all of the current designs have extremely small fields (Dimitroff and Baker, 1945). Since it would be desirable to have fairly large fields for survey purposes, an attempt was made to design an all-reflecting Schmidt camera. If the usual correcting plate of an f/1 Schmidt camera is replaced by an elliptical mirror and figure to the proper curvature, the system is essentially the same as before, except now there are no refracting surfaces involved.

Figure 1 shows a schematic diagram of the proposed system. To the first order approximation, the correcting plate can be considered to be simply a regular Schmidt surface with n = -1 and mapped into the correcting plate. If the polar coordinates of a point on the correcting plate is given by R and V, the heights of the corresponding points in the plane of the main mirror are given by,

$$h_y = R \sin V$$
$$h_x = R \cos V \sin i$$

Where i is the inclination of the sphere to corrector, V is the angle measured from the semi-major axis of the corrector in a counter-clockwise direction, R is the radial distance from the center of the ellipse. The distance of the corresponding zone of the spheroid is:

$$h = +\sqrt{h_x^2 + h_y^2}$$

Now let the vertical plane be the plane through the major axis of the corrector and the optical axis of the main mirror. Since the main mirror is a spheroid, uncorrected it suffers from spherical aberration in a plane through h and the optical axis. This plane in which the rays are contained is inclined at angle γ to the vertical plane. Then,

$$\tan\gamma = (h_y/h_x)$$
$$\text{and } \sin\gamma = (h_y/h)$$

The angle of tangency in this plane at the point (R, V)which is required to correct for the spherical aberration is demoted by a set of values of $\delta/2$ as a function of h. The angle $(-\delta)$ is the angle of departure from parallelism by rays which are sent through the system starting from the desired focal point on the optical axis. This angle can be found as a function of h by ray tracing . In order to investigate the shape of the corrector surface the tangent to the surface parallel to the major axis is usually helpful and is given by,

$$\sin\left(\frac{\delta_y}{2}\right) = \sin\gamma \sin(\delta/2)$$

and then

$$\cos\left(\frac{\delta_y}{2}\right) = \frac{\cos(\delta/2)}{\cos(\delta_y/2)}$$

The deviation $(\delta_y/2)$ is the tangent measured in the horizontal plane(through the minor axis of the corrector and the optical axis of the spheroid). If the profile in the horizontal plane is obtained as a function of the distance along the minor axis, the profile in the

plane perpendicular to the mirror parallel to the minor axis can be found through a simple transformation,

$$S_{\perp} = S(h) \cos i$$

First order theory of Schmidt surfaces (2) shows that the thickness of the Schmidt plate with n = 1 as a function of h is,

$$t = K - 1/2\left[\frac{h}{32f^2} - \frac{Eh^2}{2f^2}\right]$$

E is the distance between spheroid focus and system focus using minimal principles, E is found to have the value, $\frac{3A^2}{128f}$ (see ref 2)

$$t = K - 1/2\left[\frac{h^4}{32f^3} - \frac{3A^2h^2}{256f^3}\right]$$

Where K is the n = 0 plate thickness, f is the focal length and h = $\sqrt{h_x{}^2 + h_y{}^2}$, where h_x and h_y are rectangular coordinates on the spheroid surface. Substitution shows that,

$$h = \sqrt{R^2\sin^2 V + R^2\cos^2 V\sin^2 i}$$

$$\text{with } i = 45^{\circ},\ \sin^2 i = 1/2$$

Let h be measured in units of A and for an F/1 system f = A. The thickness for the tilted reflecting plate is,

$$t = K - \frac{\sqrt{2}}{2}\left[\frac{h^4}{32A^3} - \frac{3h^2}{256A}\right]$$

$$t = K - \frac{\sqrt{2}}{2}\left[\frac{h^4 A}{32} - \frac{3h^2 A}{256}\right]$$

$$t = K - \frac{\sqrt{2}}{2}\left[\frac{h^4}{32} - \frac{3h^2}{256}\right]$$

In one zone h runs between 0.0 and 0.5. The shape of the surface is obtained as a function of (t-K) and h. Since the previous development is approximate, larger errors may result (2). At the F/1

ratio proposed, an error of 16% underestimation of the amount of spherical aberration must be taken into account.

For an aperture, A, of the correcting plate the values of t - K for h at selected points are:

h	(t-K)
0.0 A	0.0
0.1 A	-6.96×10^{-5} A
0.2 A	-1.72×10^{-4} A
0.3 A	$+1.84\times10^{-4}$ A
0.4 A	$+2.82\times10^{-3}$ A
0.5 A	$+2.74\times10^{-3}$ A

The shape of the corrector surface for various R and V can be taken approximately from this curve. However, because the corrector is tilted, the rays coming from the upper half of the corrector do not strike quite the same zone as the lower half rays.

The error is about:

$$\Delta h \backsim 1.16(r \pm \frac{\sqrt{2}}{2}h)(\frac{1}{8}h^3 - \frac{3h}{128}) A \cos \gamma$$

Where the (+) sign is chosen if the point is above the axis and (-) if below. Δh is in units of A and r is the radius of curvature in units of A. At h = 0.4 above the axis where the aberration is nearly maximum, this is about $\Delta h \backsim -0.0032 A \cos \gamma$, or with $\gamma = 0^\circ$, $\Delta h \backsim 0.0032A$.

This error amounts to about 10% of the error produced in the completely corrected system simply with an off-axis object.

After the spherical aberration has been corrected, the other errors must be considered. The coma of the system is zero because the primary mirror is spherical. The chromatic aberration that is troublesome in ordinary Schmidt telescopes is absent.

The field of this telescops is curved. And because the correcting plate is located at the center of curvature, the radius of curvature of the plate is 1/2r.

The two remaining errors are distortion and astigmatism. (Miczaika and Sinton, 1961). Astigmatism increases with the off-axis field angle. The astigmatism is not eliminated but is usually bypassed by making the field of critical definition so that the image size is below the plate resolution for the particular focal length. Adapting the analysis already worked out(Bowen, 1961) to the present case, a table of field sizes can be worked out. The 16% error is compensated for, in the values.

(f/1 assumed)

A	D(o)	Plate Dia.	aperture obscured by plate
10 cm	46.2	8.74 cm	76%
100 cm	14.14	25.2 cm	6%
1000 cm	4.42	77.2 cm	0.5%
10,000 cm	1.41	252 cm	0.06%

In order to prevent vignetting, the diameter of the spheroid must be larger than A by an amount of twice the plate diameter. Thus for a given aperture, the corresponding primary minor diameter is given by this table.

A	D' (= dia. of Pri.)	D'/A
10 cm	27.48 cm	2.75
100 cm	150.4 cm	1.50
1000 cm	1154.4 cm	1.15
10,000 cm	10,512. cm	1.05

The optimum ratio of the apertures of the primary to correcting plate is 1.5. This means that the plate diameter cannot exceed the following values:

A	D	Plate Dia.	Present Obscuration
10 cm	15 cm	2.5 cm	6.25%
100 cm	150 cm	25 cm	6.25%
1000 cm	1500 cm	250 cm	6.25%
10,000 cm	15,000 cm	2500cm	6.25%

Because of the aperture stop (the corrector) at the radius of curvature, the distortion of the system is zero along the curved focal plane. However, if a flat plate is bent to the field curvature, then distortion will be present on the flat plate.

Because of the curious way the corrector is set up, it is necessary that the spherical mirror "see" and aperture stop at the radius of curvature. Thus, stops must be added to the system. A circular stop is first cut with aperture A; then it is bent along a diameter until one part is at a right angle with respect to the other. This aperture stop is then placed with the diameter at which the fold occurs along the minor axis of the corrector. Then the stop is rotated about the minor axis until one side points toward the minor in the horizontal plane and the other side points in a plane perpendicular to the horizontal and vertical planes. Although this arrangement produces a "four-spike" diffraction pattern, it is possible that the photographic plate holder can be mounted mechanically on this stop.

These principles can be seen better if an example is taken:

$$\text{Let } A = 100 \text{ cm at f/1}$$

$$R = 2(A) + \frac{3A^2}{128f} = 2.050A$$

The diameter of the primary spheroid is 1.5A or the primary

mirror has an 0.684 focal ratio.

R = 205 cm
A = 100 cm = minor axis of corrector
D'= 150 cm

Photographic Plate Diameter = 25 cm

A' = 144 cm = major axis of corrector
f - Ratio of primary = f/0.684
f - Ratio of System= f/1

Angular Usable field = 14°

Percentage light lost due to photographic plate = 6.25% = 0.33 stellar magnitudes.

The hypothetical design of this camera is shown in Figure 2a. A Cassegrain modification is shown in Figure 2b. It can be seen that the system is very compact and high focal ratios could be obtained with the proper reflection optics for the third mirror.

References

Dimitroff, G. and Baker, J., Telescopes and Accessories, Chapter 4, Harvard Press, 1945.

Bowen, I. S., Telescopes, ed by Kuiper and Middlehurst, Vol. I of Stars and Stellar Systems, Chapter 4, 1961.

Miczaika, G. and Sinton, W., Tools of the Astronomer, Chapter 3, Harvard Press, 1961.

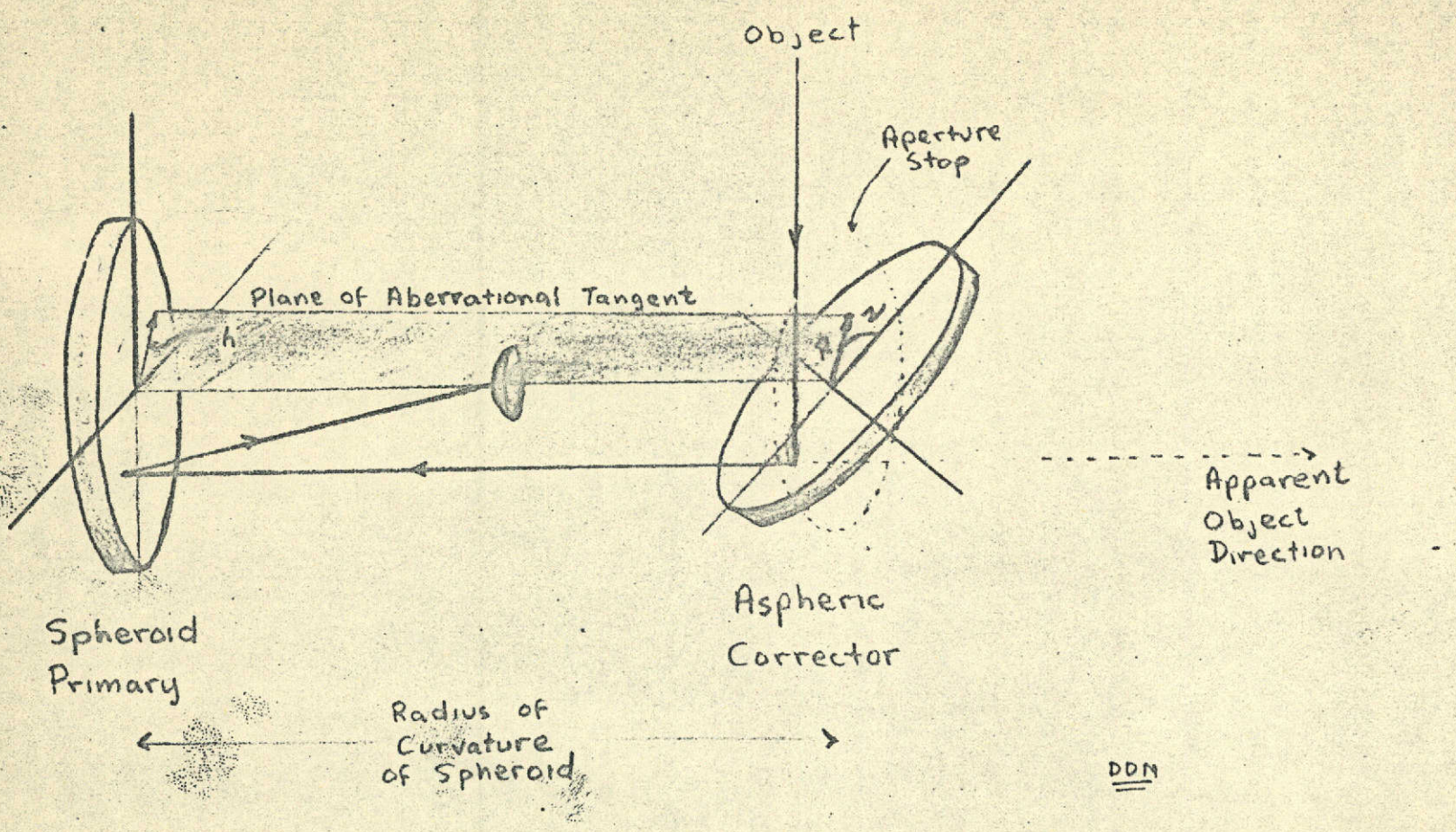

Figure 9-1 - Schematic Representation of All-Reflecting Schmidt Optics

Reproduced from best available copy.

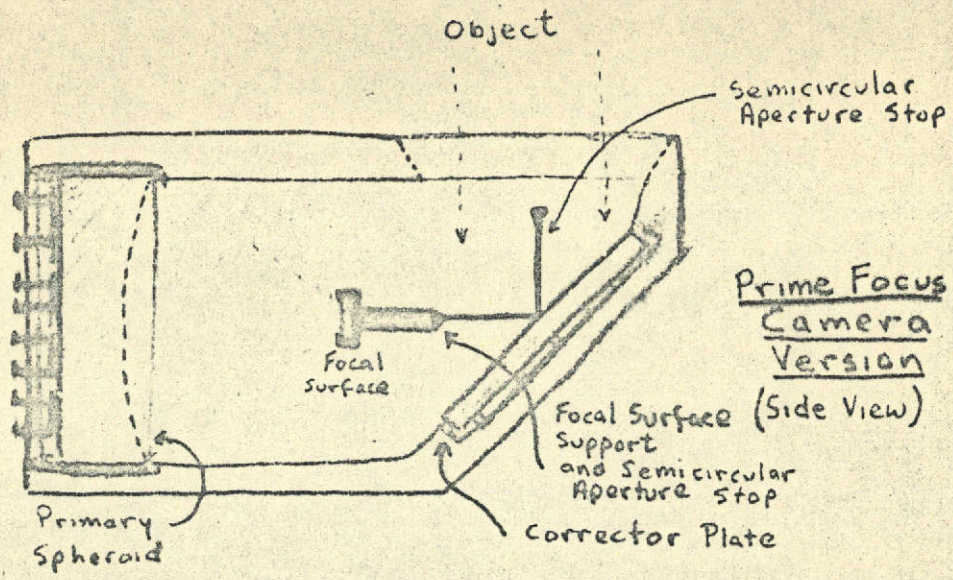

a

Prime Focus Camera Version (Side View)

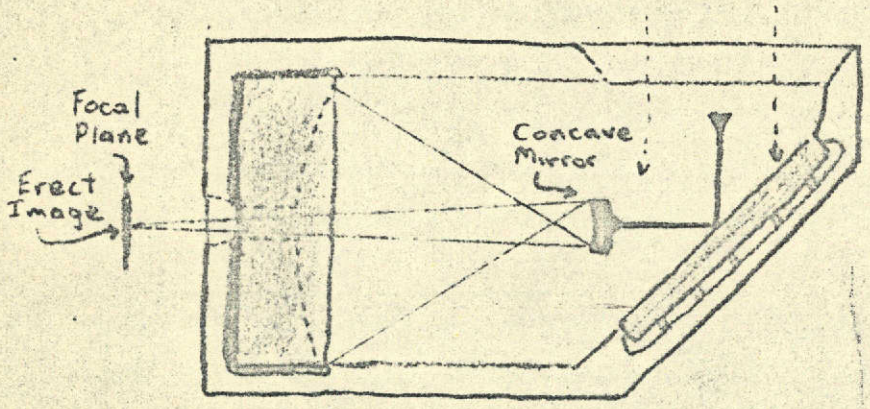

b

Gregorian Telescope Version (Side View)

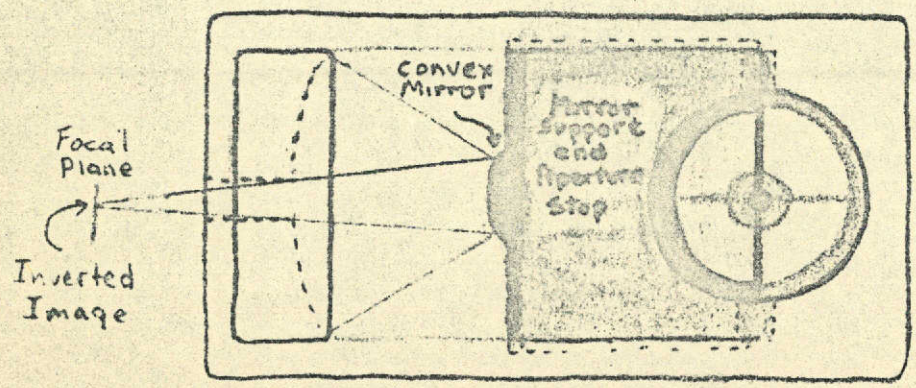

c

Cassegrain Telescope Version (Top View)

DDM

Figure 9-2. Possible Modifications of Reflecting Schmidt Optics.

Reproduced from best available copy.

Paper 10

X-ray Flux from Galactic and Extra-Galactic Sources

by G. Borse and D. Anderson

The purpose of this paper is to study possible X-ray sources in the universe and to estimate the expected flux at the top of the atmosphere. Such a study is of considerable importance at the present time for various reasons, a few of which might be mentioned. First of all an accurate determination of the atmosphere and/or corona temperature may be deduced if the X-ray flux and the optical flux are known as functions of the temperature. (Kazachevskaya and Ivanov-Kholodyni, 1960). Second, valuable information concerning the action of such radiation on the earth's atmosphere can be obtained. Lastly, rocket and satellite techniques have virtually introduced the new field of X-ray astronomy and data obtained by such means will have to be interpreted correctly.

A continuous X-ray spectrum has been observed by various workers. Friedman et al. (1960) have made extensive measurements on the X-ray flux from the sun while Giacconi, Gursky, Paolini, and Rossi (1962) have reported a detectable flux from the galactic center and from the direction of the radio sources Cygnus A and Cassiopiea. In this paper we will interpret these results and also point out other possible sources of a continuous X-ray spectrum.

According to existing theories there are a number of mechanisms available for the prediction of such a spectrum; viz., the

Compton effect, synchrotron acceleration, thermal motion of charged particles leading to non-relativistic bremsstrahlung and relativistic bremsstrahlung from fast particles. As expected, the radiation yielded by the Compton effect is quite small and has been estimated(Savedorff, 1958) to be about 10^{-6} times the radiation by other means.

The synchrotron mechanism can account for a considerable flux in the radio and visible range however, energy considerations dictate a frequency cut-off in the ultraviolet and thus prohibit radiation in the X-ray range.

The thermal motion of charged particles can account for radiation from the sun and from many stellar objects. However, this mechanism is unable to explain the flux from other sources because the high temperature $\backsim 10^6$ °K and high free electron density $\backsim 10^8 cm^{-3}$ involved (see below) are only found in stellar sources. Instead the bremsstrahlung from fast (ultra-relativistic) electrons which are available in most sources having a magnetic field can be used to estimate the X-ray flux from various thermal sources.

Thermal Radiation

We first discussed the bremsstrahlung given off by non-relativistic (thermal) electrons. Such radiation has been observed from the sun and for this reason the flux from the solar corona is first estimated. As a model we take a completely ionized hydrogen gas at a temperature of 10^6 °K with a mean free electron density (Moiseey, 1961) of $\backsim 10^8 cm^{-3}$ Assuming then, a Maxwellian distribution of

velocities we can show that about 7% of the electrons will have energies $\gtrsim$ 250 e.v. That is, these electrons will be capable of radiating in the wavelength range 10-50A. Above this range the opacity of interstellar hydrogen and helium may be so great, even for the closest stars, that no radiation will penetrate. Moreover, the peak of X-ray emission lies in this range.

The non-relativistic radiation cross-section is, (Jackson, p. 505)

(1) $x(w) \simeq \frac{16}{3} \alpha r_o^2 \frac{z^2 \hbar}{\beta^2} \ell n \frac{mv^2}{\hbar w}$

Where α= fine structure constant, r_o= classical electron radius and $\beta = v/c$. Inserting the appropriate values we find,

(2) $x(w) \simeq 4 \times 10^{-28} \hbar$

Now, the cross-section for photon production is obtained from the relation, (3) $\sigma(\hbar w)\, d(\hbar w) = x(w) \frac{dw}{\hbar w}$

whence, the integrated cross-section becomes, (4) $\sigma_t = 6 \times 10^{-24}$ cm^2

The number of photons radiated per second is then determined from, (5) $N_e = n\bar{v}.\sigma_\tau$

Where N_e = total number of electrons with energy $\gtrsim$250 e.v., n = ion density, $\bar{v}$ = mean velocity of electrons, σ_τ = integrated cross-section. Assuming that the ion density equals the electron density and taking the volume of the corona to be 3×10^{33}cm^3 we find,

1.3×10^{34} photons/sec

whence at the surface of the earth the expected flux is,

1×10^{6} photons/cm^2/sec

This result compares favorably with Friedman's (1962) reported flux of,

$$6 \times 10^{6} \text{ photons/cm}^2\text{/sec}$$
$$\text{or } 5 \times 10^{-3} \text{ ergs/cm}^2\text{/sec}$$

In a similar fashion the flux from a star can be determined. As a model we again use a fully ionized gas occupying a spherical volume with radius of 10 $R_\odot$ and a temperature of 10^{6}° K. Taking the electron density $\sim 10^{8}$ cm^{-3} and assuming this equal to the ion density and selecting the earth-star distance to 10 p.c. we find,

$$4.5 \times 10^{-4} \text{ photons/cm}^2\text{/sec}$$

A typical G star (eg. the sun) placed at the same distance would yield,

$$2.5 \times 10^{-7} \text{ photons/cm}^2\text{/sec}$$

Using these estimates as standards we obtain the figures given in Table I for a few typical stars.

Table I

Star	Spec	Distance	Intensity
β Centauri	B-1	62	1.2×10^{-5}
α Eridoni	B-5	44	2.4×10^{-5}
α Leonis	B-7	26	6.8×10^{-5}
α Centauri	G-2	1.3	1.5×10^{-5}

From these estimates we conclude that thermal radiation in the X-ray range from sources other than the sun will be negligible. We should also like to point out that the estimates given in the table are upper limits because of the high temperature that was employed. Such a high temperature, however, may be possible since it is now well known that the surface temperature of the sun

is only 6000°K whereas the coronal temperature is $\backsim 10^6$ °K.

Non-Thermal Radiation

In bright radio sources the energy radiated in the radio frequency is almost 10^3 times as much as that radiated in the visible. For thermal radiation to explain this in, for example, the Crab Nebula a temperature $\backsim 10^6$ °K and an electron concentration of $\backsim 10^4 cm^{-3}$ would be required. However, this is far greater than what is estimated by optical means; temperature $\backsim 10^5$ °K and 10^3 electrons/cm^3 (Shklovsky p. 284.). For this reason it has been postulated that the synchrotron radiation from relativistic electrons (energy $\gtrsim 10^6$ e.v.) in magnetic fields can account for the emission of radiation in the radio-frequency range.

It has been suggested (Burbidge, 1955) that these electrons originate from p-p scattering through meson production. As a result of their acceleration in the magnetic field they will pass into the relatively more dense regions of a radio source, for example, and as they traverse this medium will emit the familiar bremsstrahlung radiation which can account for a considerable X-ray flux. Such a mechanism of X-ray production has been studied extensively in the literature (Elwert, 1958, Sanedorff, 1959, and others).

The cross-section for this relativistic bremsstrahlung is given in a form suitable for our purposes by Jackson (p. 505) and the incident flux at the top of the earth's atmosphere can be estimated once the following are known:

(1) the distribution of relativistic electrons in the source.
(2) the density of heavy particles
(3) the volume of the source
(4) the earth-source distance, and
(5) the nuclear-charge of the heavy particle.

Fortunately, many of the parameters above have been estimated by optical and radio astronomical methods. (we obtained most of our data from Burbidge, 1959, and Shklovsky, 1960). Nevertheless, it should be borne in mind that such estimates are mainly heuristic and in some cases quite arbitrary.

In order to obtain the information listed in (1) we have used the well-known theory of radiation by charged particles and their distribution in the system developed by Schwinger(1949) and recast into a form suitable for astrophysics by Oort and Walraven(1956). It is sufficient for our purposes to state that the number of electrons in the energy range E to E + dE is given by the relation,

(6) $N(E)dE = KE^{-\gamma}dE$

Where N(E) is the number density of electrons per unit energy range and K and γ are constants which are determined by experimental methods. (Shklovsky, p. 191)

The particle density was estimated by comparing the mass of a heavy nucleus (Z = 10) to the density of the source when the latter was available. We found that in most cases it was sufficient to assign a particle density of 10^2 cm^{-3} for galactic objects and 1 to 10 particles/cm^3 (Z = 1) for extra galactic objects.

Using the radiation cross-section,

$$(7)\quad x(w) \sim \frac{16}{3}\ \frac{\alpha r_o^2}{\beta^2}\ Z\hbar \ln\left(2\ \frac{192}{Z^{\frac{1}{3}}}\ \frac{v}{c}\right)$$

or

$$(8)\quad x(w) \sim 2\times10^{-26} Z^2 \hbar$$

we find tha photon cross-section to be,

$$(9)\quad \sigma(\hbar)d(\hbar w) = 2\times10^{-26} Z^2\ \frac{d(\hbar w)}{\hbar w}$$

whence, the integrated cross-section for photon production in the band width 10-50 A becomes,

$$(10)\quad \sigma_T = 3.2\times10^{-26} Z^2 cm^2$$

Consequently, we deduce that the photon intensity expected at the top of the earth's atmosphere is given by,

$$(11)\quad \frac{N_e nc\,\sigma_T}{4\pi R^2} \quad \text{photons/cm}^2\text{/sec}$$

Where N_e = total number of relativistic electron in the source having an energy 10^6 e. v. ,n = density of heavy ions, c = speed of light, R = earth-source distance.

Using this relation we have obtained the figures given in Table II.

CONCLUSION:

From the results of this study we conclude that stellar objects, with the exception of the sun, because of their vast distance and weak emission, will contribute very little flux in the X-ray range at the top of the atmosphere.

On the other hand the radio sources should contribute a considerable flux. Although the background radiation is probably considerable (Giacconi et al) with a high resolution detector it is

possible to make this negligible.

The problem of interstellar absorption has not been considered; however, it has been estimated (Allen, 1959, Code, 1961) that only for radiation of about 40 Å or greater will this be appreciable.

We should also like to point out that it is not necessarily true that "bright" sources such as the Crab Nebula will yield a strong X-ray flux. Since the bramsstrahlung cross-section is approximately constant for all relativistic electrons, it is their number and not their energy which determines the rate of X-ray emission. As a result, it would be expected that although the Crab Nebula has a tremendous amount of energy, it contains no more relativistic electrons than the ancient remnants of super-nova such as IG443 and Cygnus Loop and therefore the rate of X-ray emission is approximately the same.

Recently Giacconi et al. (1962) have reported a flux of 0.6 photons/cm^2/sec from the direction of Cygnus A and Cassiopiea. Our results indicate that the origin of this flux may have been Cygnus Loop rather than the other sources, as reported. In this same paper a flux of 5 photons/cm^2/sec was also reported from the galactic center. This result compares favorably with our result of 1.46 photons/cm^2/sec.

We would like to acknowledge the interest of Dr. K. Ziock in this paper and his helpful suggestions.

Galactic Objects

	γ	K	V	Ne	N	Z	D	Flux **	Remarks
Galactic Center	2.5	3.3×10^{-17}	$7.0\times10^{66}cm^3$	$10^8/cm^3$	$10^2/cm^3$	1	8.6kpc	1.46	Mean radius of 3kpc $\rho = 10^{-23}g/cc$
IC 443	2.5	2.5×10^{-12}	$1.6\times10^{58}cm^3$	8.3×10^{-4}	10^2	10	1 kpc	0.64	mean radius 4pc
Cygnus Loop	2.6	5×10^{-15}	$2\times10^{59}cm^3$	6×10^{-6}	10^2	10	0.5kpc	0.25	
Cassiopiea	2.5	1.8×10^{-11}	6×10^{56}	9×10^{-3}	10^2	10^2	3kpc	0.03	
Crab Nebulae	2	5×10^{-9}	5×10^{55}	3×10^{-3}	10^2	10	1.1kpc	0.008	$\rho = 10^{-22}$

Extra-Galactic Objects $V = 3\times10^{64}$

Magellanic Clouds	(1) *	*	*	1.2×10^{60} (Total)	1	1	46kpc	0.0028	Mass = $6\times10^{41}g$
Cygnus A	3	3×10^{-15}	10^{68}	6×10^{-4}	20	1	7500kpc	0.0012	
NGC 4486	3	7×10^{-15}	2×10^{68}	1.4×10^{-3}	10^3	1	1.2×10^5kpc	0.0000	Mean radius $3\times10^{22}cm$ Mass = 3×10^{12} $\rho = 10^{-18}$
M31 Andromeda	(2) *	*	*	6×10^{58}	10^2	1	630kpc	8×10^{-5}	Mass = $2\times10^{44}g$

(1) No data for γ, K could be found. The minimum energy of the relativistic electrons was obtained from Burbidge and used to find the total number of related electrons.

(2) No data: same procedure as for Magellanic clouds.

** In Band 10-50Å Photons/cm^2/sec at earth

Bibliography

Allen, L. H. 1959, A. J., 64, 45.

Burbidge, G. R. 1959, Ap. J., 129, 849.

_____; Burbidge, E. M., Fowler, W., and Hoyle, F. 1955, Rev. Mod. Phys., 29, 547.

Code, A. D., 1960, A. J., 69, 393.

Elwert, E. J., 1958, J. Geophys. Res., 66, 393.

Friedman, H., 1960, Amer. J. Phys., 28, 622.

_____, 1962 "Solar X-ray Emission", The Solar Corona, ed. by Evans, J. W., Academic Press, 1963, New York, N. Y.

Giacconi, R., Gursky, Paolini, Rossi, B., 1962, Phys. Rev. Letters, No. 11.

Jackson, J. D., 1962, Classical Electrondynamics, Chap. 15, p. 505. J. Wiley and Sons, Inc., N. Y.

Kazachevskaya, T. V., Ivanov-Kholodnyi, 1959-60, Sov. Ast. A. J., 3, 937.

Moiseey, I. G., 1961, Sov. Ast. A. J., 5, No. 3.

Oort, J. H., Walraven, Th., 1956, B. A. N. 12, 285.

Savedorff, M. P., 1959, Nuovo Cimento, 13, 12.

Schwinger, J., 1949, Phys. Rev., 75, 1912.

Shklovsky, I. S., Cosmic Radio Waves, Trans. by Rodman, R. and Varsavsky, C., Harvard Univ. Press, Cambridge, Mass., 1960.

Paper 11

Residual Sky Brightness at Altitudes of 100 and 300 Miles Above the Earth

by D. Meisel

One of the principal justifications for putting astronomical telescopes in orbit above the earth is that the sky background will be less and hence longer photographic exposures could be made on very faint objects. Yet even at heights of 100 miles (161km) and 300 miles (483km), the sky is not completely dark.

On the surface of the earth the illumination of the sky background at night has the following components:

a) Scattering and absorption by lower atmospheric particles, both dust and gas.
b) Excitation and scattering in the Upper atmosphere by the gaseous component.
c) Scattering by dust, both natural and artificial, in orbit around the earth.
d) Scattering by interplanetary dust and gas.
e) Scattering and excitation in intergalactic space.
f) Contributions by unresolved celestial objects.

The effect of the lower atmosphere is to absorb and scatter light coming from above it. According to Allen(1955), a unit clear air mass at sea level diminishes the visual surface brightness by 17.05%. Thus, all visual intensities corrected for zenith distance must be further corrected by the factor,

$$I_{space} = 1.206\ I$$

In all the values quoted here the correction is included where necessary.

1. Airglow and Aurorae

At altitudes of 100 miles and 300 miles investigation shows that the only airglow left is the oxygen 6300 and 6364 forbidden transitions. Rocket measurements (Chamberlain, 1961) show that the bulk of radiation from this wavelength comes from heights above 100 miles. The actual heights are not known. A mean intensity value for the airglow contribution above 100 miles is 240 Rayleighs* for 6300 and 6364 emission (Ratcliffe, 1962). It should be noted that the airglow itself can vary in time by as much as a factor of two greater or less than the value quoted. The value is a mean for the whole sky with a three fold variation from place to place in the sky possible. In normal photometric units, the mean airglow contribution is approximately 4.2×10^{-9} lumens cm^{-2} $ster^{-1}$. The range may run from 12×10^{-9} to 1×10^{-9} for the actual values.

In addition to airglow, the aurorae may also be present from time to time, especially if the orbit is over the geomagnetic poles.

From height measurments by Stormer (1955), it is found that aurorae in the earth's shadow are most frequent between 100 and 300km. Only a few are higher than 400km. For the sunlit aurorae,

---

*One Rayleigh equals 10^6 photons striking normal to a one square centimeter surface per second.

however, the majority occur between 150 and 500km with some extending as high as 1100km. The frequency of aurorae extending higher than 300 miles is very low. Thus in order to avoid the aurora, a 300 mile altitude near the plane of the magnetic equator is the most desirable.

If for some reason, it is necessary to use a lower orbit going over the poles the intensity of a possible aurora can be reduced significantly by using the proper filters since the emissions are due to atomic lines (Ratcliffe, 1962). The intensity of the aurorae can be as much as 10^4 times brighter than the average airglow intensity. These occurences are, fortunately, very rare. Most aurorae are less than 10^2 times brighter and occupy only small portions of the sky. The frequency of aurorae depends greatly on the time of year, the time in the solar cycle, and the geomagnetic latitude and longitude. An approximate frequency relation is obtained using the following formula. The frequency of days (in percent) when an aurora is visible sometime during the night is,

$$f = 100 \exp[-0.01(|\phi_m| - 69^\circ)^2]$$

Where is the geomagnetic latitude. The principal visual auroal emissions above 100 miles are listed by decreasing intensity in the following table.

λ 6300	OI High Aurorae
6364	
5577	OI Low Aurorae
5198	NI
5200	NI
3914	N_2^+

If one compares aurorae extent with the airglow data, it seems reasonable that the λ 6300, λ 6364 emissions of airglow occur mainly between 100 miles and 400 miles high. Thus the night-glow contribution at the two heights adopted here are:

Airglow

a) 100 miles 4.2×10^{-9} lumens cm^{-2} $ster^{-1}$
b) 300 miles 0.9×10^{-9} lumens cm^{-2} $ster^{-1}$

Aurorae

a) 100 miles 10^{-7} to 10^{-5} lumens cm^{-2} $ster^{-1}$
b) 300 miles 10^{-8} to 10^{-10} lumens cm^{-2} $ster^{-1}$

2. Geocorona and Geo-dust Cloud

In addition to airglow and aurora, there is also scattering of sunlight by particles and electrons in the space around the earth out to 300,000 miles. The main contribution to the scattering is that by electrons. Molecular or atomic scattering is negligible because of the low density. Calculation shows that using data obtained by rocket and satellites (Ratcliffe, 1962) for electron densities give 3×10^{14} free electrons between 100 miles and 100,000 miles. With each electron scattering $\sim 10^{-27}$ of the sun's radiation, the average aurface brightness is given in terms of angle from the sun θ by the approximate formula,

$$I_e(\theta)(\text{lumens cm}^{-2}\text{ ster}^{-1}) = 0.25 \times 10^{-9}(1-\cos\theta) \quad \text{(at 100 miles)}$$

The recently discovered dust cloud around the earth (Sky and Telescope, 1961) can be shown by similar calculations to contribute

to the brightness of the sky. However, in this regard, the estimates and assumptions are much less certain. With particles of 2μ diameter, densities on the order of 10^{-11} particles per cm^3 and a reflectivity of 10%, the visual brightness contributed in lumens cm^{-2} $ster^{-1}$ is given by the formula:

$$I_d(0) = 1.5 \times 10^{-13} \ (1-\cos\theta)$$

This contribution is several powers of ten below the electron contribution and may be neglected.

The average contributions at the specified altitudes adopted are given below.

Geocorona and Dust

100 miles 0.5×10^{-9} lumens cm^{-2} $ster^{-1}$
300 miles 0.4×10^{-9} lumens cm^{-2} $ster^{-1}$

These quantities may be variable but nothing definite regarding this is available. The values adopted should be reasonable estimates.

3. Artificial Particle Belts

Of importance to our present considerations is the effect of scattering by artificial dust belts put into orbit for communication purposes.

In a recent experiment, the surface brightness of such a belt occupying an area $0.^{\circ}3$ by 10° was 2% above the normal terrestrial dark sky or about 31×10^{-9} $lumens^{-2}$ $ster^{-1}$. If the belt spreads out as is planned then the contribution will be about

0.05×10^{-9} lumens cm^{-2} $ster^{-1}$ over an area $360^{\circ} \times 2^{\circ}$. If the cloud fails to disperse properly the band could pose quite a problem as it sweeps through the field. If more than one belt is launched, as seems likely, the brightness which could be contributed might be as much as 0.1×10^{-9} lumens cm^{-2} sec^{-1}. More recent measurements (Science Vol. 141, No. 3583, Aug. 30, 1963) show that the interference of furthur West Ford experiments may truly be great, perhaps as much as 100 or 1000 times the amount quoted above.

4. The Zodiacal Light

Beyond distances of 200,000 miles, there is a contribution to the night sky brightness from interplanetary dust called the zodiacal light. The intensity of the light depends on the angular distance from the sun, and the ecliptic latitude. Recent measurements by Peterson (1961) agree well with the values given by Allen (1955). The brightness distribution is approximated by,

$$I_z = [B_o(\lambda - \theta)]\, e^{-0.69 \frac{\tan \beta}{\tan \beta}} + K_\beta$$

Where β is the ecliptic latitude of the direction, λ is the ecliptic longitude and θ is the longitude of the sun. B_o and $I(\lambda - \theta)$ are given by the following tables adopted from Allen (1955).

K_β is the contribution of $I(\beta, \lambda)$ at $\beta = 90^\circ$ which is found to be 2.0×10^{-9} lumens cm^{-2} $ster^{-1}$ (Allen, 1955)

$I(\lambda - \odot)$ in units of 10^{-9} lumens cm^{-2} $ster^{-1}$

$(\lambda - \odot)$	10°	20°	30°	40°	50°	60°	70°	90°	110°	130°	150°	170°	180°
$I(\lambda - \odot)$	1560	318	120	72	48	36	26	169	12	10.3	11.2	13.5	15.8

$(\lambda - \odot)$	30°	40°	60°	90°	130°	180°
β_o	25°	31°	36°	50°	70°	40°

5. Galactic Light

In addition to the light coming from interplanetary matter, there is a significant amount of light coming from the stars, dust and gas within our own galaxy. This light comes from two sources. One source is unresolved background stars and the other is from luminous material between the stars.

In the case of unresolved stars, attempts have been made to utilize star counts and extrapolate these to obtain integrated star intensities. One of the more recent attempts was made by Roach and Megill (1961). It can be shown that when interstellar absorption is present, extrapolations will give results that are too high. Out of the galactic plane, the star count method should be more reliable as the amount of dust is definitely decreased.

A somewhat more reliable method to use at present for low galactic latitudes is photoelectric monitoring of the galactic regions. The intensity of the light from the galactic plane including

that from stars fainter than 8^m and galactic material was investigated by Elsasser and Haug (1960). Like the zodiacal light the galactic contribution can be approximated by:

$$I_g(b^I, \ell^I) = I(b)^{-0.69} \frac{\tan b^I}{\tan b_o^I} + K_b^I \ell^I$$

Where b^I is the old system galactic latitude, ℓ^I is the old system galactic longitude and $I(b^I)$ and b_o^I are taken from the tables that follow. $Kb^I \ell^I$ is the value of $I(b^I \ell^I)$ at the galactic poles. The tables give the values obtained from the results of Elsasser and Haug (1960) and corrected for extinction. These results at specific positions agree well with the average quoted by Allen (1955).

Table A

ℓ	0°	30°	60°	90°	120°	150°	180°
I	19.8	20.3	21.9	16.2	13.1	15.8	19.8
ℓ	180°	210°	240°	270°	300°	330°	360°
I	19.8	21.5	19.4	21.0	32.8	59.4	19.8

Where $I(b, \ell)$ is in units of 10^{-9} lumens cm^{-2} $ster^{-1}$

Table B

ℓ	0°	30°	60°	90°	120°	150°	180°
b_o	5	15	20	20	10	10	15
ℓ	180°	210°	240°	270°	300°	330°	360°
b_o	15	20	20	10	20	20	5

The value of K^I, ℓ^I is derived from the Roach and Megill (1961) values at $b^I = 90°$ which is in good agreement with the value quoted by Allen (1955) and is found to be,

2.7×10^{-9} lumens $cm^{-2} ster^{-1}$

6. Unresolved Extragalactic Nebulae

In a manner similar to that used to extrapolate star counts, de Vaucouleurs (1948, 1949) estimated the intensity from unresolved galaxies as a mere 0.06×10^{-9} lumens $cm^{-2} ster^{-1}$. It is interesting to note that this is about the same contribution as the dust cloud of artificial particles would have when dispersed uniformly in orbit. Both of these have about the same contribution which is minor compared to the others.

Under normal conditions, in the visual region of the spectrum, the sky brightness at the galactic pole will have the following approximate values,

100 miles* $I = 9.46 \times 10^{-9}$ lumens $cm^{-2} ster^{-1}$
300 miles $I = 6.06 \times 10^{-9}$ lumens $cm^{-2} ster^{-1}$

These represent 32% and 20% of the normal sea level zenith sky as defined by Allen (1955).

These values represent the minimum that should be present most of the time. For a telescope at an altitude of 500 miles, the value is reduced 5.2 so there is little real advantage to having a telescope in orbit at this altitude at least from the standpoint of sky brightness. There is some advantage for the 300 mile altitude as it results in a fair reduction of auroral and airglow interference.

---

*If the 6300 lines are filtered out, the intensity is the same as 300 miles.

7. Monochromatic Intensities

It is desirable in this study to try to find monochromatic intensities at various wavelengths from the ultraviolet through the infrared. The color-intensity relationship for the terrestrial night sky in the visual region has been investigated (see Allen, 1955). However, this is not sufficient for our purpose. According to Allen (1955) the color index of the night sky is about +0.5 giving a color temperature of 5000° K.

The lumen, however, is based on a color temperature of 2000° K so a transformation must be made. In addition, a lumen is defined as the flux seen by the "standard" human eye rather than the energy emitted by the source. The conversion between the two systems involves evaluation of these integrals,

$$\int_{\lambda_1}^{\lambda_2} I(\lambda, T_1)\, E(\lambda)\, d\lambda = \int_{\lambda_1}^{\lambda_2} I(\lambda, T_2)\, E(\lambda)\, d\lambda$$

Where $E(\lambda)$ is the sensitivity function of the eye and $I(\lambda T)$ is the intensity function at the given temperature T.

In the visual region for $T_1 = 2000^\circ K$ the integral on the left becomes for one lumen of flux,

$$\int_{\lambda_1}^{\lambda_2} I(\lambda, T_2)\, E(\lambda)\, d\lambda = 1.5 \times 10^4 \text{ ergs sec}^{-1}\text{cm}^{-2}$$

Integrating the left side, it can be shown that,

$$\int_{\lambda_1}^{\lambda_2} I(\lambda, T_2)\, E(\lambda)\, d\lambda = 1_{\lambda\ \max}\, \phi(\lambda, T_2)\, E(\lambda)\, d\lambda$$

Thus upon substitution,

$$I(\lambda \max, T_2) = \frac{1.5 \times 10^4 \text{ ergs sec}^{-1}\text{cm}^{-2}}{\int_{\lambda_1} \phi^{\lambda 2}(\lambda, T_2)\, E(\lambda)\, d\lambda}$$

Suppose $\phi(\lambda, T_2)$ is the relative intensity from the Plank function, then the integral may be evaluated. Let $T_2 = 5000^{\circ}K$ then it is found that,

$$I(\lambda \max, T_2 = 5000^{\circ}K) = 3.6 \text{ ergs sec}^{-1}\text{cm}^{-2}\,\text{A}^{\circ -1}$$
(for one lumen with $T = 5000^{\circ}K$)

The monochromatic intensity at other wavelengths is given by,

$$I(\lambda T_2) = (\lambda\ T_2) I(\lambda \max)$$

Tables of $\phi(\lambda, T_2)$ are available as functions of λT so that the intensity under the blackbody assumption can be found.

There is a slight deviation from the blackbody assumption for the unresolved star component which must be taken into account. Because of interstellar dust, more stars are visible in the red of the spectrum than the blue, hence the total contribution is somewhat higher in the red than in the blue.

In Table I, the computed monochromatic intensities corrected for the above effect have been listed. If a curve of these values is constructed, the intensity in any particular wavelength range may be approximated. These are for the galactic pole. Values at other places in the sky may be found by using the simple ratios $(I\mu / \mu)$ for that position as conversion factors.

It should be kept in mind that the values of the sky brightness quoted and those obtained from the formulae are approximations only. No consideration is given to the discontinuities which may

exist because of absorption by atoms and molecules. Their profiles are not accurately known for the sky background and consideration of this is beyond the scope of this work.

Table I
Background continuum contribution
at 100 and 300 miles altitude*

μ	I_e	I_p
0.1	4.3×10^{-15}	2.1×10^{-4}
0.2	2.6×10^{-10}	24.4
0.3	0.45×10^{-8}	6.8×10^{2}
0.4	1.26×10^{-8}	2.56×10^{3}
0.5	1.85×10^{-8}	4.68×10^{3}
0.6	2.05×10^{-8}	6.22×10^{3}
0.7	1.97×10^{-8}	7.01×10^{3}
0.8	1.80×10^{-8}	7.29×10^{3}
0.9	1.57×10^{-8}	7.12×10^{3}
1.0	1.37×10^{-8}	6.92×10^{3}
1.2	1.00×10^{-8}	6.08×10^{3}
1.4	0.74×10^{-8}	5.24×10^{3}
1.6	0.55×10^{-8}	4.45×10^{3}
1.8	3.81×10^{-8}	3.81×10^{3}
2.0	0.32×10^{-8}	3.23×10^{3}
2.2	0.25×10^{-8}	2.77×10^{3}
2.4	0.20×10^{-8}	2.42×10^{3}
3.0	0.11×10^{-8}	1.67×10^{3}
4.0	0.05×10^{-8}	1.01×10^{3}

I_e in ergs/cm^{-2}/ster^{-1}sec^{-1} A and I_p in photons/cm^{-2}sec^{-1} ster^{-1}0A

Note: the atomic lines at λ 6300 from nightglow contribute $\sim3\times10^{3}$ photons cm^{-2} sec^{-1}ster^{-1} at 6300 and $\sim10^{3}$ at λ 6364.

*These values are the minimum at the galactic pole. Intensities at the galactic equator are about 10^{2} higher than the values quoted. In the zodiacal band at less than 40° from the sun, the factor rises to 10^{3} times greater than the above values.

References

Allen, C. W., Astrophysical Quantities, Althone Press, (1955)

Chamberlain, J. W. Physics of the Aurorae and Airglow, Academic Press, New York, 1962.

Elsässer H. and Haug, U., Zs. f.Ap. 50, 121, (1960).

Peterson, Alan W. Ap. J. 133, 668, (1961).

Ratcliffe, J. A., Physics of the Upper Atmosphere, Academic, (1962).

Roach, F. E. and Megill, L. R., Ap. J. 133, 228, (1961).

Sky and Telescope, Vol 21, p. 71, (1961).

Störmer, C., "The Polar Aurorae", Clarenden Press (1955).

Paper 12

Star Count Deviations as an Indicator of Star to Dust Ratios

by D. Meisel

Two independent means of obtaining the sky background contribution have been attempted recently. The first by Roach and Megill [1] consists of a numerical extrapolation and subsequent integration of the Groningen Observatory star counts[2]. The second method is that employed by Elsässer and Haug using photoelectric observations [3]:

By comparing the two studies, one finds that the integration gives values that are on the average too high compared to observation. How does one explain this, assuming of course no gross accidental errors? The following is a possible explanation.

In the star count method, the basic integral is:

$$N_{m,\ell,b} = \int_{m=m_o}^{\infty} \phi_{\ell b}(m)dm$$

Where ℓ = galactic longitude, α = galactic latitude, and m = apparent magnitude. If there were no absorption, the integral should give the same value as the integral in which ϕ is affected by absorption of finite extent.

$$\int_{m_o}^{\infty} \phi_{\ell b}(m)dm = \int_{m_o}^{\infty} \phi_{\ell b}(m)dm$$

The star density at any particular magnitude m is given by a function over all absolute magnitudes,

$$\phi(m) = \int_{-\infty}^{\infty} \phi\,(m, M)dM$$

But $M = m-5-5\log r-A(r)$, differentiating and substituting;

$$\phi(m) = \int_0^\infty \phi(m,r)\left[\frac{-11.6}{r} \quad \frac{\partial A(r)}{\partial r}\right]dr$$

If $A(r) = 0$ then,

$$\phi_o(m) = \int_0^\infty \frac{-k\,\phi(m,r)}{r}dr$$

Thus, $\phi(m) = \phi_o(m) - \int_0^\infty \phi(m,r)\frac{A(r)}{r}\,dr$

$\phi(m,r)$ is the <u>actual</u> space distribution of all stars of apparent magnitude m. Now,

$$N_m = \int_m^\infty \phi(m)dm =$$

$$\int_0^\infty \phi(m)dm - \int_m^\infty \int_0^\infty \phi(m,r)\frac{\partial A(r)}{\partial r}\,drdm$$

$$N_m = N_{mo} \int_m^\infty \int_0^\infty \phi(m,r)\frac{\partial A(r)}{\partial r}\,drdm$$

If $A(r) = K_o e^{-r/\beta}$ then

$$N_m = N_{mo} + \int_m^\infty \int_0^\infty \frac{K_o e^{-r/\beta}}{\beta}\,\phi(m,r)drdm$$

$\bar{K}$ is a mean absorption coefficient and $\beta \; 1/\bar{K}\rho$ and since,

$$\frac{d(\log N_m)}{dm} = \frac{1}{Nm}\frac{dN_m}{dm}$$

we have,

$$\frac{dN_m}{dm} = \frac{dN_{mo}}{dm} + \int_0^\infty \frac{K_o e^{-r/\beta}}{\beta}\,\phi(m,r)dr$$

The integral is positive for $\phi(m,r) > O$. Thus absorption tends to increase the slope when $\frac{dN_{om}}{dm}$ is + and tends to decrease it when $\frac{dN_{mo}}{dm}$ is (-). The case for constant $\phi(m,r)$ is:

a) In an extrapolation for $\frac{dN_{mo}}{dm}$ positive, the slope will be <u>too</u>

large so the integral will be too large. If the absorption is such that β is small then the slope very much increased, if β is large then the slope is increased less.

If $\frac{dN_{mo}}{dm}$ is negative, then a small β will make the slope less negative and again the extrapolation will give too large a value. If β is large, then the extrapolation will be too large but to a lesser extent.

Now $\phi(m, r) = C \int_0^{\rho}(r)\, 4\pi r^2 dr$

If $\rho(r)$ is such that $\int_0^{\infty} \phi(m, r)$ is constant, then the slope difference $\int_0 e^{-r/\beta}\, dr = \beta$ depends on β alone. If $\phi(m, r) \propto r^n$ where n is an integer, then

$$\int_0^{\infty} r^n e^{-r/\beta} dr = \beta^{n+1} n!$$

Thus the larger n gets, the greater the effect of changes in β. If $\phi(m, r)$ increases logarithmically, then the difference in slope is a constant. If $\rho(r)$ were such that $\phi(m, r)\, r^{-n} n > 0$ then the integral is always negative and so the slope will tend to give values upon extrapolation which will be too small.

In most regions β and $\phi(m, r)$ will increase in the same direction so that deviations from the integral will be nearly constant.

If ϕ / β is high then the regions are relatively dust laden. If ϕ / β is low, the regions are relatively dust free. If ϕ / β is smaller than the average, then the departure from some mean value of the integral will be, $\Delta N = (N_{obs} - \bar{N})$ and will be negative.

If ϕ / β is larger than average, then $\Delta N = (N_{obs} - \bar{N})$ will be positive.

The fact that absorption is present will make the intensity computed greater than that observed, since the slope with absorption is less than that without absorption. If the computed intensity is much greater than the observed mean value is, then it is an indication that ϕ / β is high or relatively dust free. If ϕ/β is low, then the computed intensity is not much greater than the observed. If this hypothesis is correct, one would expect the more negative (EH-Gr43)* values to correspond to the dust laden areas and hence correspond to the areas of greatest polarization. The other regions where (EH-Gr43) is positive, are relatively dust free. Examination of the Hα regions of the southern Milky Way show the maximum concentration of strong negative values are concentrated within H α regions.

In the southern hemisphere:

a) the strongest polarization occurs for $B = 0^\circ$ $\ell = 270^\circ$, with minima at $B = 0^\circ$, ℓ 260° and 290°
b) The strongest Hα occur at $\ell = 270^\circ$ and 290°
c) The greatest negative EH-Gr43 value occurs at $\ell = 240^\circ$ which is within strong polarization, but little H α .

---

* Elsässer and Haug values minus Gronigen 43 values.

b) The strongest Hα occurs at $\ell = 270^{\circ}$
c) The greatest negative EH - Gr43 value occurs at $\ell = 240^{\circ}$ which is within strong polarization, but Hα.
d) The next strongest are located at $\ell = 270^{\circ}$ within very strong polarization with H and then at $\ell = 290^{\circ}$ which again coincides with strong Hα and polarization.

In regions where the (EH - Gr43) values are positive, gas emission exceeds dust contribution.

References

Elsässer, H. and Haug, U., Zs. f. Ap. 50, 121, (1960)

Groningen Publications, No. 43

Roach, F. and Megill, L., Ap. J. 133, 228, 1961